

Scattering data and bound states of a squeezed double-layer structure

Alexander V. Zolotaryuk and Yaroslav Zolotaryuk

Bogolyubov Institute for Theoretical Physics, National Academy of Sciences of Ukraine, Kyiv 03143, Ukraine

E-mail: azolo@bitp.kiev.ua, yzolo@bitp.kiev.ua

Abstract. A heterostructure composed of two parallel homogeneous layers is studied in the limit as their widths l_1 and l_2 , and the distance between them r shrinks to zero simultaneously. The problem is investigated in one dimension and the squeezing potential in the Schrödinger equation is given by the strengths V_1 and V_2 depending on the layer thickness. A whole class of functions $V_1(l_1)$ and $V_2(l_2)$ is specified by certain limit characteristics as l_1 and l_2 tend to zero. The squeezing limit of the scattering data $a(k)$ and $b(k)$ derived for the finite system is shown to exist only if some conditions on the system parameters V_j , l_j , $j = 1, 2$, and r take place. These conditions appear as a result of an appropriate cancellation of divergences. Two ways of this cancellation are carried out and the corresponding two resonance sets in the system parameter space are derived. On one of these sets, the existence of non-trivial bound states is proven in the squeezing limit, including the particular example of the squeezed potential in the form of the derivative of Dirac's delta function, contrary to the widespread opinion on the non-existence of bound states in δ' -like systems. The scenario how a single bound state survives in the squeezed system from a finite number of bound states in the finite system is described in detail.

Keywords: one-dimensional quantum systems, point interactions, resonant tunneling, bound states.

1. Introduction

Exactly solvable models are used in quantum mechanics to describe the properties of realistic physical systems such as scattering coefficients, bound states, etc. in closed form using elementary functions. A whole class of these models is represented by Schrödinger operators with singular zero-range potentials defined on the sets consisting of isolated points. In the literature these operators are referred to as contact or *point interaction* models (see books [1, 2, 3, 4] for details and references).

Berezin and Faddeev [5] were the first who realized a point interaction, restricting first the free Hamiltonian to functions defined outside the point of singularity, then constructed self-adjoint extensions of the obtained symmetric operator. Later, numerous publications (see, e.g., publications [3, 4, 6, 7, 8, 9, 10, 11, 12, 13, 14, 15, 16], a few to mention) were devoted to this standard construction of point interactions using the theory of self-adjoint extensions of symmetric operators. An interesting approach based on the integral form of the one-dimensional Schrödinger equation has been developed by Lange [17, 18] with some revision of Kurasov's theory [6].

Another approach is to approximate the singular potential part of the formal Schrödinger equation by regular finite-range functions and to study the convergence in the norm-resolvent topology [19, 20]. Thus, Cheon and Shigehara [21] were the first who developed an approach how to construct a whole family of point interactions from shrinking three separated Dirac's delta potentials to one point, using various potential strengths. Next, in spite of that Šeba [19], using a general regularization of the derivative of Dirac's delta function $\beta\delta'(x)$ ($\beta \in \mathbb{R}$ is a strength constant) as a potential part in the one-dimensional Schrödinger equation, has constructed the point interaction which is opaque *everywhere* on the γ -axis, for some particular regularizing sequences of $\delta'(x)$, the perfect reflection was observed [22, 23, 24, 25, 26] *almost everywhere* on the β -axis. In other words, a partial transmission of particles through the potential $\beta\delta'(x)$ was shown to occur at certain isolated points $\{\beta_n\}$ forming a set of Lebesgue's measure zero depending on the regularizing sequence. In general terms, for a whole class of regularizing sequences of the potential $\beta\delta'(x)$, Golovaty and coworkers [27, 28, 29, 30] have rigorously proved the existence of a *resonance set* in the β -space and its dependence on the regularization. On this set, they constructed the algorithm for computing the matrix that connects the two-sided boundary conditions at the point of singularity and allows to calculate the reflection-transmission coefficients.

Besides 'pure' single-point interactions, more specified models, which are important in applications, have been elaborated. Thus, the potential $V(x) = \alpha\delta(x) + \beta\delta'(x)$, $\alpha < 0$, $\beta \in \mathbb{R}$, has been used by Gadella *et al.* as a perturbation of the background potentials such as the harmonic oscillator [31] or the infinite square well [32]. The spectrum of a one-dimensional V-shaped quantum well perturbed by three types of a point impurity as well as three solvable two-dimensional systems (the isotropic harmonic oscillator, a square pyramidal potential and their combination) perturbed by a point potential centered at the origin has been studied by Fassari *et al.* in the recent papers [33, 34, 35].

Some aspects of the so-called δ' -interaction, its approximations by local and non-local potentials as well as its combination with background potentials, have been investigated by Albeverio and coworkers [36, 37, 38, 39, 40].

Two-point interactions are also important in applications. The resonant tunnelling through double-barrier scatters is still an active area of research for the applications to nanotechnology [41, 42]. Tunnelling times in double-barrier point potentials and the associated questions such as the generalized version of the Hartman effect have been studied in [43, 44, 45, 46, 47]. Another important aspect regarding the application of double-point potentials is the Casimir effect that arises in the behaviour of the vacuum energy between two homogeneous parallel plates. For the interpretation of this effect, Muñoz-Castañeda and coworkers [48, 49, 50, 51, 52] reformulated the theory of self-adjoint extensions of symmetric operators over bounded domains in the framework of quantum field theory. Particularly, they have calculated the vacuum energy and identified which boundary conditions generate attractive or repulsive Casimir forces between the plates.

The present paper is devoted to the investigation of a planar heterostructure composed of two extremely thin layers separated by a small distance in the limit as both the layer thickness and the distance between the layers simultaneously shrink to zero. The electron motion in this system is supposed to be confined in the longitudinal direction (say, along the x -axis) being perpendicular to the transverse planes where electronic motion is free. The three-dimensional Schrödinger equation of such a structure can be separated into longitudinal and transverse parts, resulting in the reduced stationary one-dimensional Schrödinger equation

$$-\psi''(x) + V(x)\psi(x) = E\psi(x) \quad (1)$$

with respect to the longitudinal component of the wave function $\psi(x)$ and the electron energy E . Here, $V(x)$ is a potential for electrons to be specified below for a double-layer structure and the prime stands for the differentiation over x . Concerning numerical computations, we note that equation (1) has been written in the system for which $\hbar^2/2m^* = 1$ where m^* is an effective electron mass. In the calculations we set $m^* = 0.1 m_e$ where m_e is the free electron mass, so in our case $1 \text{ eV} = 2.62464 \text{ nm}^{-2}$.

The potential $V(x)$ in equation (1) is understood as a sequence of regular potentials that shrinks to a point. It is not necessary for this sequence to have any well-defined limit even in the sense of distributions for producing a point interaction. Thus, ignoring any condition for the existence of a distributional limit, one can extensively enlarge the family of regularizing sequences. Thus, for a double-layer structure, the resonance set consist of curves that covers the corresponding resonance set for the δ' -potential formed by the points lying on these curves [53, 54, 55]. Another aspect of this approach is the possibility to investigate in a squeezing limit the resonant-tunnelling transmission through biased potentials [56, 57, 58].

The goal of this article is to construct the family of point interactions from a double-layer potential as this potential shrinks to a point. The approach is based on the analysis

of the scattering data $a(k)$ and $b(k)$, ($k := \sqrt{E}$), in a squeezing limit. In general, the functions $a(k)$ and $b(k)$ diverge in this limit, however, at some constraints on the system parameters, a cancellation of divergences may happen, leading to the existence of finite values for the scattering data.

The definition of the scattering data $a(k)$ and $b(k)$ is given in the next section. Here, the relationship of these data with the transmission matrix for a single-layer structure is discussed. The scattering data for a double-layer structure are present in section 3. Two types of resonance sets are found in the next section as the result of cancellation of divergences. The behaviour of bound states in a squeezing limit is described in section 5. In the next section, the three-scale power-connecting parametrization of the double-layer potential is applied for the numerical illustration of the behaviour of bound states and wave functions under the squeezing procedure. Finally, some concluding remarks are discussed in section 7.

2. Preliminaries

In this section we present the definitions of the scattering functions $a(k)$ and $b(k)$, and some relations regarding the transmission matrix, reflection-transmission coefficients and bound states of a single-layer structure.

2.1. Monodromy matrix

For equation (1) we define two sets of linearly independent solutions to this equation as follows

$$\begin{aligned} \phi_1(x) &\sim e^{-ikx}, & \phi_2(x) &\sim e^{ikx} & \text{as } x \rightarrow -\infty, \\ \psi_1(x) &\sim e^{-ikx}, & \psi_2(x) &\sim e^{ikx} & \text{as } x \rightarrow +\infty. \end{aligned} \quad (2)$$

This pair of solutions can be coupled through the monodromy matrix \mathbf{M} as

$$\text{col}\{\phi_1(x), \phi_2(x)\} = \mathbf{M} \text{col}\{\psi_1(x), \psi_2(x)\}, \quad (3)$$

where

$$\mathbf{M} = \begin{pmatrix} a(k) & b(k) \\ b^*(k) & a^*(k) \end{pmatrix}, \quad \det \mathbf{M} = |a|^2 - |b|^2 = 1. \quad (4)$$

On the other hand, one can write

$$\text{col}\{\psi_1(x), \psi_2(x)\} = \mathbf{M}^{-1} \text{col}\{\phi_1(x), \phi_2(x)\}, \quad (5)$$

where

$$\mathbf{M}^{-1} = \begin{pmatrix} a^*(k) & -b(k) \\ -b^*(k) & a(k) \end{pmatrix}. \quad (6)$$

2.2. Reflection-transmission coefficients and equations for bound states

The reflection-transmission coefficients for an incident plane wave from the right are defined by

$$\psi(x) = \begin{cases} T_r e^{-ikx} & \text{as } x \rightarrow -\infty, \\ e^{-ikx} + R_r e^{ikx} & \text{as } x \rightarrow +\infty \end{cases} \quad (7)$$

and, from the comparison with the expression of the matrix \mathbf{M} given by equations (3) and (4), we obtain

$$R_r = b(k)/a(k), \quad T_r = 1/a(k). \quad (8)$$

Then the equation for bound states reads $a(i\kappa) = 0$.

Similarly, the reflection-transmission coefficients for an incident plane wave from the left are defined by

$$\psi(x) = \begin{cases} e^{ikx} + R_l e^{-ikx} & \text{as } x \rightarrow -\infty, \\ T_l e^{ikx} & \text{as } x \rightarrow +\infty \end{cases} \quad (9)$$

and, from the comparison with the expression for the matrix \mathbf{M}^{-1} given by equations (5) and (6), we obtain

$$R_l = -b^*/a, \quad T_l = 1/a. \quad (10)$$

In this case the equation for bound states reads $a^*(-i\kappa) = 0$.

2.3. Transmission matrix and its relation to a monodromy matrix

For a finite-range system supported on the interval $x_1 \leq x \leq x_2$, for which $V(x) \equiv 0$ on the intervals $-\infty < x < x_1$ and $x_2 < x < +\infty$, the transmission matrix Λ is defined by the matrix equation

$$\begin{pmatrix} \psi(x_2) \\ \psi'(x_2) \end{pmatrix} = \Lambda \begin{pmatrix} \psi(x_1) \\ \psi'(x_1) \end{pmatrix}, \quad \Lambda = \begin{pmatrix} \lambda_{11} & \lambda_{12} \\ \lambda_{21} & \lambda_{22} \end{pmatrix}, \quad \det \Lambda = 1, \quad (11)$$

for both positive- ($k > 0$) and negative-energy ($k = i\kappa$) solutions of equation (1). Note that in both these cases, the elements λ_{ij} 's are real-valued functions of k or $i\kappa$.

In general, the Λ -matrix can be defined as follows. Let $u(x)$ and $v(x)$ be linearly independent solutions of the Schrödinger equation (1) for a layer placed on the interval $x_1 \leq x \leq x_2$. Then one can express the elements λ_{ij} in terms of the initial values of these solutions in the following form:

$$\begin{aligned} \lambda_{11} &= W(x_1)^{-1} [u(x_2)v'(x_1) - u'(x_1)v(x_2)], \\ \lambda_{12} &= W(x_1)^{-1} [u(x_1)v(x_2) - u(x_2)v(x_1)], \\ \lambda_{21} &= W(x_1)^{-1} [u'(x_2)v'(x_1) - u'(x_1)v'(x_2)], \\ \lambda_{22} &= W(x_1)^{-1} [u(x_1)v'(x_2) - u'(x_2)v(x_1)], \end{aligned} \quad (12)$$

where $W(x_1) = u(x_1)v'(x_1) - u'(x_1)v(x_1) = W(x)$, $x_1 \leq x \leq x_2$, is the Wronskian of equation (1). Equations (12) are simplified if the solutions $u(x)$ and $v(x)$ satisfy the initial conditions at one of the ends $x = x_1$ or $x = x_2$. Let

$$u(x_1) = 1, \quad u'(x_1) = 0, \quad v(x_1) = 0, \quad v'(x_1) = 1. \quad (13)$$

Then, using these values in equations (12), one immediately finds

$$\Lambda = \begin{pmatrix} u(x_2) & v(x_2) \\ u'(x_2) & v'(x_2) \end{pmatrix}, \quad \det \Lambda = 1. \quad (14)$$

Similarly, the solution to equation (1) can also be expressed in terms of the functions $u(x)$ and $v(x)$ defined by initial conditions (13). Let $\psi(x_1)$ and $\psi'(x_1)$ be boundary conditions at $x = x_1$. Then this solution on the interval $x_1 \leq x \leq x_2 < \infty$ reads

$$\psi(x) = \psi(x_1)u(x) + \psi'(x_1)v(x). \quad (15)$$

The scattering data $a(k)$ and $b(k)$ can be expressed via the elements of the Λ -matrix defined on the interval $x_1 \leq x \leq x_2$. To this end, consider representation (2) for the solution $\phi_1(x)$, writing

$$\phi_1(x) = \begin{cases} e^{-ikx}, & -\infty < x < x_1, \\ a(k)e^{-ikx} + b(k)e^{ikx}, & x_2 < x < +\infty. \end{cases} \quad (16)$$

Inserting the values of this function and its derivatives at $x = x_1$ and $x = x_2$ into the equations

$$\begin{aligned} \phi_1(x_2) &= \lambda_{11}\phi_1(x_1) + \lambda_{12}\phi_1'(x_1), \\ \phi_1'(x_2) &= \lambda_{21}\phi_1(x_1) + \lambda_{22}\phi_1'(x_1), \end{aligned} \quad (17)$$

and solving the resulting pair of equations with respect to $a(k)$ and $b(k)$, we immediately find

$$a(k) = \frac{D(k)}{2}e^{ik(x_2-x_1)}, \quad b(k) = \frac{p(k) - iq(k)}{2}e^{-ik(x_1+x_2)}, \quad (18)$$

where

$$D := \lambda_{11} + \lambda_{22} - i(k\lambda_{12} - k^{-1}\lambda_{21}), \quad p := \lambda_{11} - \lambda_{22}, \quad q := k\lambda_{12} + k^{-1}\lambda_{21}. \quad (19)$$

Using the equation $\det \Lambda = 1$, one can derive the equality $|D|^2 = 4 + p^2 + q^2$ and, as a result, for positive-energy solutions ($k = \sqrt{E}$), the relation $\det \mathbf{M} = 1$ holds true. In a squeezed limit, one can set $x_1 \rightarrow -0$ and $x_2 \rightarrow +0$, so that $a(k) = D/2$ and $b(k) = (p - iq)/2$.

The equation for bound states reads $a(i\kappa) = 0$ and, as a result, from (18) with (19) we get the following general equation given in terms of the Λ -matrix elements:

$$\lambda_{11}(\kappa) + \lambda_{22}(\kappa) + \kappa\lambda_{12}(\kappa) + \kappa^{-1}\lambda_{21}(\kappa) = 0. \quad (20)$$

This is a general equation given in terms of the elements of the Λ -matrix.

3. Transmission matrix, scattering data and wave functions for a double-layer potential

Consider the system consisting of two separated layers described by the piecewise constant potential, which is defined on the whole axis as follows

$$V(x) = \begin{cases} V_1, & 0 < x < l_1, \\ V_2, & l_1 + r < x < l_1 + l_2 + r, \\ 0 & -\infty < x < 0, \quad l_1 < x < l_1 + r, \quad l_1 + l_2 + r < x < \infty. \end{cases} \quad (21)$$

Here $V_j \in \mathbb{R}$ (barrier if $V_j > 0$ or well if $V_j < 0$), $l_j > 0$ (layer thickness) and $r > 0$ (distance between layers), $j = 1, 2$.

On each of the three intervals $0 < x < l_1$, $l_1 < x < l_1 + r$ and $l_1 + r < x < l_1 + r + l_2$, the corresponding transmission matrices, denoted by Λ_1 , Λ_0 , Λ_2 , respectively, can be written immediately on the basis of general formula (14). Thus, setting $x_1 = 0$ and $x_2 = l_1$ for Λ_1 , $x_1 = l_1$ and $x_2 = l_1 + r$ for Λ_0 , $x_1 = l_1 + r$ and $x_2 = l_1 + r + l_2$ for Λ_2 , we have

$$\Lambda_j = \begin{pmatrix} \cos(k_j l_j) & k_j^{-1} \sin(k_j l_j) \\ -k_j \sin(k_j l_j) & \cos(k_j l_j) \end{pmatrix}, \quad \Lambda_0 = \begin{pmatrix} \cos(kr) & k^{-1} \sin(kr) \\ -k \sin(kr) & \cos(kr) \end{pmatrix}, \quad (22)$$

with $k_j = \sqrt{k^2 - V_j}$, $j = 1, 2$. Then the total transmission matrix is the product $\Lambda = \Lambda_2 \Lambda_0 \Lambda_1$ with the elements

$$\begin{aligned} \lambda_{11} &= [\cos(k_1 l_1) \cos(k_2 l_2) - (k_1/k_2) \sin(k_1 l_1) \sin(k_2 l_2)] \cos(kr) \\ &\quad - [(k_1/k) \sin(k_1 l_1) \cos(k_2 l_2) + (k/k_2) \cos(k_1 l_1) \sin(k_2 l_2)] \sin(kr), \\ \lambda_{12} &= [(1/k_1) \sin(k_1 l_1) \cos(k_2 l_2) + (1/k_2) \cos(k_1 l_1) \sin(k_2 l_2)] \cos(kr) \\ &\quad + [(1/k) \cos(k_1 l_1) \cos(k_2 l_2) - (k/k_1 k_2) \sin(k_1 l_1) \sin(k_2 l_2)] \sin(kr), \\ \lambda_{21} &= -[k_1 \sin(k_1 l_1) \cos(k_2 l_2) + k_2 \cos(k_1 l_1) \sin(k_2 l_2)] \cos(kr) \\ &\quad - [k \cos(k_1 l_1) \cos(k_2 l_2) - (k_1 k_2/k) \sin(k_1 l_1) \sin(k_2 l_2)] \sin(kr), \\ \lambda_{22} &= [\cos(k_1 l_1) \cos(k_2 l_2) - (k_2/k_1) \sin(k_1 l_1) \sin(k_2 l_2)] \cos(kr) \\ &\quad - [(k/k_1) \sin(k_1 l_1) \cos(k_2 l_2) + (k_2/k) \cos(k_1 l_1) \sin(k_2 l_2)] \sin(kr). \end{aligned} \quad (23)$$

Setting $x_1 = 0$ and $x_2 = l_1 + l_2 + r$ in equations (18) and (19), where the Λ -matrix elements are given by equations (23), we find the scattering data:

$$\begin{aligned} \frac{a(k)}{\cos(k_1 l_1) \cos(k_2 l_2)} &= \left\{ e^{-ikr} - \frac{i}{2} \left[\left(\frac{k}{k_1} + \frac{k_1}{k} \right) t_1 + \left(\frac{k}{k_2} + \frac{k_2}{k} \right) t_2 \right] e^{-ikr} \right. \\ &\quad \left. + \frac{1}{2} \left[i \left(\frac{k^2}{k_1 k_2} + \frac{k_1 k_2}{k^2} \right) \sin(kr) - \left(\frac{k_1}{k_2} + \frac{k_2}{k_1} \right) \cos(kr) \right] t_1 t_2 \right\} e^{ik(l_1 + l_2 + r)}, \end{aligned} \quad (24)$$

$$\begin{aligned} \frac{b(k)}{\cos(k_1 l_1) \cos(k_2 l_2)} &= \frac{i}{2} \left\{ \left(\frac{k_1}{k} - \frac{k}{k_1} \right) t_1 e^{ikr} + \left(\frac{k_2}{k} - \frac{k}{k_2} \right) t_2 e^{-ikr} \right. \\ &\quad \left. + \left[\left(\frac{k^2}{k_1 k_2} - \frac{k_1 k_2}{k^2} \right) \sin(kr) + i \left(\frac{k_1}{k_2} - \frac{k_2}{k_1} \right) \cos(kr) \right] t_1 t_2 \right\} e^{-ik(l_1 + l_2 + r)}, \end{aligned} \quad (25)$$

where $t_j := \tan(k_j l_j)$, $j = 1, 2$.

A family of *one*-point interactions can be realized from equation (1) with potential (21) if all the three size parameters l_1, l_2 and r converge to the origin $x = 0$, whereas the values $|V_1|$ and $|V_2|$ (and therefore $|k_1|$ and $|k_2|$) must tend to infinity. However, the arguments of trigonometric functions $k_1 l_1$ and $k_2 l_2$ in equations (23) must be finite (including zero) in the limit as $l_1, l_2 \rightarrow 0$. Therefore one can consider a whole family of functions $V_1 = V_1(l_1)$ and $V_2 = V_2(l_2)$, for which the arguments will be finite. To this end, let us define the function set $\mathcal{G} = \mathcal{G}_1 \times \mathcal{G}_2$ with

$$\mathcal{G}_j := \{V_j(l_j) \mid \lim_{l_j \rightarrow 0} |V_j(l_j)|^{1/2} l_j = c_j\}, \quad j = 1, 2, \quad (26)$$

where the constants c_1 and c_2 are finite or zero ($0 \leq c_j < \infty$). Since the constants c_j 's can be either non-zero or zero, the four cases of \mathcal{G} should be considered separately: $\mathcal{G}_{11}(c_1 > 0, c_2 > 0)$, $\mathcal{G}_{01}(c_1 = 0, c_2 > 0)$, $\mathcal{G}_{10}(c_1 > 0, c_2 = 0)$, $\mathcal{G}_{00}(c_1 = 0, c_2 = 0)$.

Let us analyze first the asymptotic behaviour of the elements λ_{11} and λ_{22} in (23) as $l_1, l_2, r \rightarrow 0$. They will be finite and non-zero if

$$\begin{aligned} |V_1(l_1)/V_2(l_2)| &\rightarrow \text{const.} > 0 && \text{for } \mathcal{G}_{11}, \\ |V_1(l_1)| |V_2(l_2)|^{-1/2} l_1 &\rightarrow \text{const.} \geq 0, \quad |V_2(l_2)|^{1/2} l_1 &\rightarrow \text{const.} \geq 0 && \text{for } \mathcal{G}_{01}, \\ |V_1(l_1)|^{-1/2} |V_2(l_2)| l_2 &\rightarrow \text{const.} \geq 0, \quad |V_1(l_1)|^{1/2} l_2 &\rightarrow \text{const.} \geq 0 && \text{for } \mathcal{G}_{10}, \\ |V_1(l_1)| l_1 l_2 &\rightarrow \text{const.} \geq 0, \quad |V_2(l_2)| l_1 l_2 &\rightarrow \text{const.} \geq 0 && \text{for } \mathcal{G}_{00}, \end{aligned} \quad (27)$$

and the distance r shrinks to zero sufficiently fast compared with the squeezing of l_1 and l_2 , so that each of the following expressions:

$$\begin{aligned} |V_1(l_1)|^{1/2} r, |V_2(l_2)|^{1/2} r & \quad (\mathcal{G}_{11}), \quad |V_1(l_1)| l_1 r, |V_2(l_2)|^{1/2} r & \quad (\mathcal{G}_{01}), \\ |V_1(l_1)|^{1/2} r, |V_2(l_2)| l_2 r & \quad (\mathcal{G}_{10}), \quad |V_1(l_1)| l_1 r, |V_2(l_2)| l_2 r & \quad (\mathcal{G}_{00}), \end{aligned} \quad (28)$$

must converge to an arbitrary constant or zero. Using the definition of the \mathcal{G} -sets, from conditions (27) one can derive asymptotic relations between $l_1 \rightarrow 0$ and $l_2 \rightarrow 0$ in the form of ratios

$$\frac{l_1}{l_2} (\mathcal{G}_{11}), \frac{|V_1(l_1)| l_1}{|V_2(l_2)|^{1/2}} (\mathcal{G}_{01}), \frac{|V_1(l_2)| l_2}{|V_1(l_1)|^{1/2}} (\mathcal{G}_{10}), \frac{|V_1(l_1)| l_1}{|V_2(l_2)| l_2} (\mathcal{G}_{00}) \rightarrow \text{const.} > 0, \quad (29)$$

which are required to converge to arbitrary *non-zero* constants. Under these conditions, one can check that limits (27) indeed take place. For instance, for the \mathcal{G}_{01} -set, we have $|V_2|^{1/2} l_1 = |V_1| l_1^2 |V_2|^{1/2} / |V_1| l_1 \rightarrow 0$ as required. Next, e.g., owing to the last ratio in (29), $|V_1| l_1 l_2 = \text{const.} |V_2| l_2^2 \rightarrow 0$ for the \mathcal{G}_{00} -set. Having the asymptotic relative behaviour of l_1 and l_2 given by expressions (29), now one can derive asymptotic relations $r = r(l_1)$ or $r = r(l_2)$ fulfilling limits (28). Thus, using these limits as well as the definition of the \mathcal{G} -sets, under the requirement that expressions

$$\frac{r}{l_1} (\mathcal{G}_{11}), \frac{r}{l_2} (\mathcal{G}_{01}), \frac{r}{l_1} (\mathcal{G}_{10}), |V_1(l_1)| l_1 r (\mathcal{G}_{00}) \rightarrow \text{const.} \geq 0, \quad (30)$$

have to converge to arbitrary (positive) constants or zero, we are convinced that conditions (28) hold true.

Thus, under the conditions imposed on the asymptotic behaviour of the parameters l_1, l_2, r as they converge to the origin in the way described by relations (29) and (30) having finite limits, the limit Λ -matrix elements λ_{11} and λ_{22} are finite and non-zero. For each of the $\mathcal{G} = \{\mathcal{G}_{11}, \mathcal{G}_{01}, \mathcal{G}_{10}, \mathcal{G}_{00}\}$ -sets, all these convergence ways $\{l_1, l_2, r\} =: \gamma \rightarrow 0$ can be interpreted respectively as *pencils of paths* $\Gamma = \{\Gamma_{11}, \Gamma_{01}, \Gamma_{10}, \Gamma_{00}\}$ in the $\{l_1, l_2, r\}$ -space with the vertex located at the origin, so that any path $\gamma \in \Gamma$ provides finite non-zero limits of λ_{11} and λ_{22} . Since $|k_j| \rightarrow \infty$ in the limit as $\gamma \rightarrow 0$, we have $\lambda_{12} \rightarrow 0$, while λ_{21} in general diverges as $\gamma = \{l_1, l_2, r\} \rightarrow 0$. Therefore the two-sided boundary conditions on the wave function $\psi(x)$ in this limit are of the Dirichlet type:

$$\psi(\pm 0) = 0 \quad \text{if } |\lambda_{21}| \rightarrow \infty. \quad (31)$$

This is a particular case of the second part of the Albeverio-Dąbrowski-Kurasov (ADK) theorem [7], regarding *separated* point interactions. However, under some constraints on

the limit (resonance) constants of the expressions listed in (29) and (30), the squeezing limit of λ_{21} may be finite or zero and in this case we are dealing with the first part of the ADK theorem, when the resulting point interactions are *non-separated*. The corresponding jump conditions at $x = 0$ on the wave function $\psi(x)$ and its derivative $\psi'(x)$ will be given below in an explicit form.

Finally, on the basis of equation (15), the wave function as a solution of equation (1) with potential (21) can easily be computed explicitly using the linearly independent solutions obeying initial conditions (13) on each of the intervals: $0 \leq x \leq l_1$, $l_1 \leq x \leq l_1 + r$, $l_1 + r \leq x \leq l_1 + l_2 + r$. Thus, on the whole axis $-\infty < x < \infty$, the positive-energy solution describing an incident plane wave from the right with asymptotic representation (16) reads

$$\phi_1(x) = \begin{cases} \varphi_l(x) := e^{-ikx}, & -\infty < x < 0, \\ \varphi_1(x) := \cos(k_1x) - i(k/k_1) \sin(k_1x), & 0 < x < l_1, \\ \varphi_0(x) := \varphi_1(l_1) \cos[k(x - l_1)] \\ \quad + k^{-1} \varphi_1'(l_1) \sin[k(x - l_1)], & l_1 < x < l_1 + r, \\ \varphi_2(x) := \varphi_0(l_1 + r) \cos[k_2(x - l_1 - r)] \\ \quad + k_2^{-1} \varphi_0'(l_1 + r) \sin[k_2(x - l_1 - r)], & l_1 + r < x < l_1 + l_2 + r, \\ \varphi_r(x) := a(k)e^{-ikx} + b(k)e^{ikx}, & l_1 + l_2 + r < x < \infty. \end{cases} \quad (32)$$

Setting in these formulas $k = i\kappa$, we obtain the wave function corresponding to the discrete spectrum and the bound energy levels κ 's are found from the equation $a(i\kappa) = 0$. In this case, the last formula in (32) reads $\varphi_r(x) = b(i\kappa) \exp(-\kappa x)$.

4. Resonance sets for the existence of scattering data and a bound state in a squeezed limit

Consider an asymptotic representation of equations (24) and (25) in the limit as $\gamma \rightarrow 0$. Expanding $\exp(\pm ikr) = 1 \pm ikr + \mathcal{O}(r^2)$ in the curly brackets of these equations and omitting the terms which vanish in the limit as $\gamma \rightarrow 0$, one can write the following asymptotic representation of the scattering data:

$$a(k) \simeq \frac{1}{2} \left[z_1(k) + z_2(k) - \frac{i}{k} \Delta(k) \right] \cos(k_1 l_1) \cos(k_2 l_2) e^{ik(l_1 + l_2 + r)}, \quad (33)$$

$$b(k) \simeq \frac{1}{2} \left[z_1(k) - z_2(k) + \frac{i}{k} \Delta(k) \right] \cos(k_1 l_1) \cos(k_2 l_2) e^{-ik(l_1 + l_2 + r)}, \quad (34)$$

where

$$z_1(k) := 1 - k_1 t_1 r - (k_1/k_2) t_1 t_2, \quad z_2(k) := 1 - k_2 t_2 r - (k_2/k_1) t_1 t_2 \quad (35)$$

and

$$\Delta(k) := k_1 t_1 + k_2 t_2 - k_1 t_1 k_2 t_2 r. \quad (36)$$

The function $\Delta(k)$ is the most singular term and it diverges in general as $\gamma \rightarrow 0$. However, under certain conditions imposed on the system parameters, this term may

be finite if a squeezing procedure is carried out in a proper way. This happens if a cancellation of divergences occurs in this term. Indeed, such a cancellation procedure does exist if a squeezed limit is arranged in the two ways as follows. The first way is to set $\Delta(k) = 0$, where the distance r participates in the cancellation. The second way is to suppose that $r \rightarrow 0$ sufficiently fast, available to suppress the divergent product $k_1 k_2$ in the last term of (36). In this case, only the first two terms in (36) must be canceled out.

4.1. The first way of the cancellation of divergences

Using the condition $\Delta(k) = 0$ and the expressions for $z_1(k)$ and $z_2(k)$ given by equations (35), one can establish that

$$\begin{aligned} \left(1 - k_1 t_1 r - \frac{k_1}{k_2} t_1 t_2\right) \cos(k_1 l_1) \cos(k_2 l_2) &= -\frac{k_1 \sin(k_1 l_1)}{k_2 \sin(k_2 l_2)} \\ &= \frac{\cos(k_1 l_1) - k_1 r \sin(k_1 l_1)}{\cos(k_2 l_2)} = \frac{\cos(k_1 l_1)}{\cos(k_2 l_2) - k_2 r \sin(k_2 l_2)} =: \theta(k) \end{aligned} \quad (37)$$

and furthermore

$$\left(1 - k_2 t_2 r - \frac{k_2}{k_1} t_1 t_2\right) \cos(k_1 l_1) \cos(k_2 l_2) = \theta^{-1}(k). \quad (38)$$

In order to prove equations (37), we rewrite the condition $\Delta(k) = 0$ [see equation (36)] as the following three equations:

$$k_1 t_1 r = 1 + \frac{k_1 t_1}{k_2 t_2}, \quad \frac{k_1}{k_2} = k_1 t_2 r - \frac{t_2}{t_1}, \quad k_1 = \frac{k_2 t_2}{t_1 (k_2 t_2 r - 1)}. \quad (39)$$

Inserting then the right-hand sides of these equations into the term $z_1(k)$ multiplied by $\cos(k_1 l_1) \cos(k_2 l_2)$, we get the right-hand expressions of (37), respectively. Similarly, inserting the right-hand sides of the relations

$$k_2 t_2 r = 1 + \frac{k_2 t_2}{k_1 t_1}, \quad \frac{k_2}{k_1} = k_2 t_1 r - \frac{t_1}{t_2}, \quad k_2 = \frac{k_1 t_1}{t_2 (k_1 t_1 r - 1)}, \quad (40)$$

which follow from the same equation $\Delta(k) = 0$, into the term $z_2(k)$ multiplied by $\cos(k_1 l_1) \cos(k_2 l_2)$, one obtains the inverse expressions to those in (37), i.e., $\theta^{-1}(k)$ defined by (38). Using next relations (37) and (38) in equations (33) and (34), one immediately finds

$$a(k) \simeq \frac{1}{2} [\theta(k) + \theta^{-1}(k)] e^{ik(l_1 + l_2 + r)}, \quad b(k) \simeq \frac{1}{2} [\theta(k) - \theta^{-1}(k)] e^{-ik(l_1 + l_2 + r)}. \quad (41)$$

One can easily see that $\det \mathbf{M} = 1$ and $a(k)$, $b(k)$ are well-defined functions.

In the equation $\Delta(k) = 0$ [see definition (36)], all the three terms diverge in a squeezing limit. Multiplying this equation by $r \rightarrow 0$, in the limit as $\gamma \rightarrow 0$, we obtain the equation

$$A_1 + A_2 = A_1 A_2, \quad (42)$$

where

$$A_j := \lim_{\gamma \rightarrow 0} (k_j t_j r) = \begin{cases} f_j \tan \sigma_j & \text{if } k_j l_j \rightarrow \sigma_j \neq 0, \\ \eta_j & \text{if } k_j l_j \rightarrow 0, \end{cases} \quad (43)$$

with

$$f_j := \lim_{\gamma \rightarrow 0} (k_j r) \quad \text{and} \quad \eta_j := \lim_{\gamma \rightarrow 0} (k_j^2 l_j r) \quad j = 1, 2. \quad (44)$$

Here $\sigma_j \in \mathbb{R} \cup \mathbb{I}$ (σ_j is either real or imaginary and $|\sigma_j| = c_j$, the constants used for the definition of the \mathcal{G} -sets). Due to definition (43), equation (42) contains the four particular cases: (i) $\sigma_j \neq 0$, $j = 1, 2$, (ii) $k_1 l_1 \rightarrow 0$, $\sigma_2 \neq 0$, (iii) $\sigma_1 \neq 0$, $k_2 l_2 \rightarrow 0$ and (iv) $k_j l_j \rightarrow 0$, $j = 1, 2$. The solutions to these equations define the following four resonance sets, which are subsets of the Γ -sets:

$$\begin{aligned} X_{11} &:= \{\gamma \in \Gamma_{11} \mid f_1 \tan \sigma_1 + f_2 \tan \sigma_2 = f_1 f_2 \tan \sigma_1 \tan \sigma_2\}, \\ X_{01} &:= \{\gamma \in \Gamma_{01} \mid \eta_1 = (\eta_1 - 1) f_2 \tan \sigma_2\}, \\ X_{10} &:= \{\gamma \in \Gamma_{10} \mid \eta_2 = (\eta_2 - 1) f_1 \tan \sigma_1\}, \\ X_{00} &:= \{\gamma \in \Gamma_{00} \mid \eta_1 + \eta_2 = \eta_1 \eta_2\}. \end{aligned} \quad (45)$$

It follows from these equations that the resonance sets $X = \{X_{11}, X_{01}, X_{10}, X_{00}\}$ do not depend on k . According to equations (37), on these sets the limit element θ is given by

$$\theta = \begin{cases} (\cos \sigma_1 - f_1 \sin \sigma_1) / \cos \sigma_2 = \cos \sigma_1 / (\cos \sigma_2 - f_2 \sin \sigma_2) \\ \quad = -f_1 \sin \sigma_1 / f_2 \sin \sigma_2, & X_{11}, \\ (1 - \eta_1) / \cos \sigma_2 = 1 / (\cos \sigma_2 - f_2 \sin \sigma_2) = -\eta_1 / f_2 \sin \sigma_2, & X_{01}, \\ \cos \sigma_1 - f_1 \sin \sigma_1 = \cos \sigma_1 / (1 - \eta_2) = -f_1 \sin \sigma_1 / \eta_2, & X_{10}, \\ 1 - \eta_1 = 1 / (1 - \eta_2) = -\eta_1 / \eta_2, & X_{00}, \end{cases} \quad (46)$$

being real, which does not depend on k as well. Therefore the limit scattering data $a(k)$ and $b(k)$ also do not depend on k , so that no bound states exist on these resonance sets. Due to asymptotic representation (41), the scattering data are

$$a = \frac{1}{2}(\theta + \theta^{-1}), \quad b = \frac{1}{2}(\theta - \theta^{-1}), \quad (47)$$

with θ given by equations (46).

As follows from equations (32), in the squeezed limit we have the boundary values $\phi_1(-0) = 1$, $\phi_1(+0) = a + b = \theta$ and $\phi_1'(-0) = -ik$, $\phi_1'(+0) = ik(b - a) = -ik\theta^{-1}$. Similar relations take place for $\phi_2(x) = \phi_1^*(x)$ and thus for any function $\psi(x)$ as a linear combination of $\phi_1(x)$ and $\phi_2(x)$, the jump conditions read

$$\psi(+0) = \theta \psi(-0), \quad \psi'(+0) = \theta^{-1} \psi'(-0). \quad (48)$$

4.2. The second way of the cancellation of divergences

Here the cancellation of divergences occurs if $k_1 t_1 + k_2 t_2 = 0$ and the last term in (36) will be finite in each of the limits $\gamma \rightarrow 0$. Then from the expression $\Delta(k) \simeq (k_1 t_1)^2 r = (k_2 t_2)^2 r$ follows that the terms $k_1 t_1 r^{1/2}$ and $k_2 t_2 r^{1/2}$ are also finite in this limit. Therefore

the terms $k_1 t_1 r$ and $k_2 t_2 r$ must disappear in any $\gamma \rightarrow 0$ limit and therefore they can be ignored in expressions (35). Thus, we have the equation

$$\Delta(k) = -k_1 t_1 k_2 t_2 r = (k_1 t_1)^2 r = (k_2 t_2)^2 r \quad (49)$$

and the asymptotic representation

$$z_1(k) \simeq 1 - (k_1/k_2)t_1 t_2, \quad z_2(k) \simeq 1 - (k_2/k_1)t_1 t_2. \quad (50)$$

Using next these relations in equations (33) and (34), one immediately finds

$$a(k) \simeq \frac{1}{2} \left[\theta(k) + \theta^{-1}(k) + \frac{i}{k} \alpha(k) \right] e^{ik(l_1+l_2+r)}, \quad (51)$$

$$b(k) \simeq \frac{1}{2} \left[\theta(k) - \theta^{-1}(k) - \frac{i}{k} \alpha(k) \right] e^{-ik(l_1+l_2+r)}, \quad (52)$$

where

$$\theta(k) = \frac{\cos(k_1 l_1)}{\cos(k_2 l_2)} = -\frac{k_1 \sin(k_1 l_1)}{k_2 \sin(k_2 l_2)}, \quad \alpha(k) = k_1 k_2 r \sin(k_1 l_1) \sin(k_2 l_2). \quad (53)$$

Multiplying the equation $k_1 t_1 + k_2 t_2 = 0$ by $r^{1/2}$, instead of equation (42) we obtain the equation

$$B_1 + B_2 = 0, \quad (54)$$

where

$$B_j := \lim_{\gamma \rightarrow 0} (k_j t_j r^{1/2}) = \begin{cases} g_j \tan \sigma_j & \text{if } k_j l_j \rightarrow \sigma_j \neq 0, \\ \beta_j & \text{if } k_j l_j \rightarrow 0. \end{cases} \quad (55)$$

Here

$$g_j := \lim_{\gamma \rightarrow 0} (k_j r^{1/2}) \quad \text{and} \quad \beta_j := \lim_{\gamma \rightarrow 0} (k_j^2 l_j r^{1/2}). \quad (56)$$

Equation (54) together with (55) and (56) defines the following four resonance sets being subsets of the Γ -sets:

$$\begin{aligned} Y_{11} &:= \{\gamma \in \Gamma_{11} \mid g_1 \tan \sigma_1 + g_2 \tan \sigma_2 = 0\}, \\ Y_{01} &:= \{\gamma \in \Gamma_{01} \mid \beta_1 + g_2 \tan \sigma_2 = 0\}, \\ Y_{10} &:= \{\gamma \in \Gamma_{10} \mid g_1 \tan \sigma_1 + \beta_2 = 0\}, \\ Y_{00} &:= \{\gamma \in \Gamma_{00} \mid \beta_1 + \beta_2 = 0\}. \end{aligned} \quad (57)$$

According to (53), on the resonance sets $Y = \{Y_{11}, Y_{01}, Y_{10}, Y_{00}\}$, we have

$$\theta = \begin{cases} \cos \sigma_1 / \cos \sigma_2 = -g_1 \sin \sigma_1 / g_2 \sin \sigma_2, & Y_{11}, \\ 1 / \cos \sigma_2 = -\beta_1 / g_2 \sin \sigma_2, & Y_{01}, \\ \cos \sigma_1 = -g_1 \sin \sigma_1 / \beta_2, & Y_{10}, \\ 1 = -\beta_1 / \beta_2, & Y_{00}, \end{cases} \quad (58)$$

and

$$\alpha = \begin{cases} g_1 g_2 \sin \sigma_1 \sin \sigma_2, & Y_{11}, \\ \beta_1 g_2 \sin \sigma_2, & Y_{01}, \\ g_1 \beta_2 \sin \sigma_1, & Y_{10}, \\ \beta_1 \beta_2, & Y_{00}. \end{cases} \quad (59)$$

Then, according to (51) and (52), we obtain

$$a(k) = \frac{1}{2} \left(\theta + \theta^{-1} + \frac{i}{k} \alpha \right), \quad b(k) = \frac{1}{2} \left(\theta - \theta^{-1} - \frac{i}{k} \alpha \right), \quad (60)$$

where the limit elements θ and α are defined by equations (58) and (59). Similarly to (46), the limit expressions for θ and α do not depend on k .

In the case of scattering data (60), from equations (32) in the squeezed limit we have $\phi_1(-0) = 1$, $\phi_1(+0) = a(k) + b(k) = \theta$ and $\phi_1'(-0) = -ik$, $\phi_1'(+0) = ik [b(k) - a(k)] = -ik\theta^{-1} + \alpha$. Similarly, $\phi_2(-0) = 1$, $\phi_2(+0) = a^*(k) + b^*(k) = \theta$ and $\phi_2'(-0) = ik$, $\phi_2'(+0) = ik [a^*(k) - b^*(k)] = ik\theta^{-1} + \alpha$. Therefore, for any function $\psi(x)$ from the continuum spectrum, the jump conditions read

$$\psi(+0) = \theta \psi(-0), \quad \psi'(+0) = \theta^{-1} \psi'(-0) + \alpha \phi_1(-0). \quad (61)$$

One can check that these equations hold true for the eigenfunctions from the discrete spectrum as well. Indeed, from equation $a(i\kappa) = 0$ we obtain the relation $\theta + \theta^{-1} + \alpha/\kappa = 0$ and, as a result, the boundary values $\phi_1(-0) = 1$, $\phi_1(+0) = b(i\kappa) = \theta$, $\phi_1'(-0) = \kappa$, $\phi_1'(+0) = -\kappa b(i\kappa) = -\kappa\theta = \kappa\theta^{-1} + \alpha$. Similar values take place for $\phi_2(x)$ and $\phi_2'(x)$, so that equations (61) also take place for the bound states.

4.3. Existence of a single bound state

Consider equations (60). From the equation $a(i\kappa) = 0$ we find the bound state level κ and the value for $b(k)$ at this level:

$$\kappa = -\frac{\alpha}{\theta + \theta^{-1}}, \quad b(i\kappa) = \theta. \quad (62)$$

More explicitly, inserting expressions (58) and (59) into equation (62) and using definition (57), the bound state level as a function given on the resonance Y -sets can be expressed through one of the following formulas:

$$\begin{aligned} \kappa|_{Y_{11}} &= -\frac{g_1 g_2 \tan \sigma_1 \tan \sigma_2}{\cos^{-2} \sigma_1 + \cos^{-2} \sigma_2} = \frac{g_1^2 \tan^2 \sigma_1}{\cos^{-2} \sigma_1 + \cos^{-2} \sigma_2}, \\ \kappa|_{Y_{01}} &= \frac{\beta_1^2}{1 + \cos^{-2} \sigma_2} = \frac{(\beta_1 g_2)^2}{\beta_1^2 + 2g_2^2}, \\ \kappa|_{Y_{10}} &= \frac{\beta_2^2}{1 + \cos^{-2} \sigma_1} = \frac{(g_1 \beta_2)^2}{2g_1^2 + \beta_2^2}, \\ \kappa|_{Y_{00}} &= -\frac{1}{2} \beta_1 \beta_2 = \frac{1}{2} \beta_1^2 = \frac{1}{2} \beta_2^2. \end{aligned} \quad (63)$$

The level κ is an unique set function with non-trivial values only on the resonance Y -sets.

5. Convergence of the multiple bound states of a finite-thickness system to a squeezed bound state

Equations (62) and (63) describe the *single* bound state, which as a set function, is non-trivial only on the resonance Y -sets. These equations have been derived under the

squeezing of a structure with finite thickness. On the other hand, any structure with the potential having a well of sufficient depth admits the existence of several number of bound states. Therefore it would be reasonable to analyze the behaviour of all the bound states in a squeezing limit. To this end, we start from the equation $a(i\kappa) = 0$ in which $a(k)$ is given by expression (24), resulting in the equation $F(\kappa) = 0$ with

$$F(\kappa) = \left[2 + \left(\frac{\kappa}{k_1} - \frac{k_1}{\kappa} \right) t_1 + \left(\frac{\kappa}{k_2} - \frac{k_2}{\kappa} \right) t_2 \right] (1 + t_0) + \left[\left(\frac{\kappa^2}{k_1 k_2} + \frac{k_1 k_2}{\kappa^2} \right) t_0 - \left(\frac{k_1}{k_2} + \frac{k_2}{k_1} \right) \right] t_1 t_2, \quad (64)$$

where $t_j := \tan(k_j l_j)$, $j = 1, 2$, and $t_0 := \tanh(\kappa r)$. The function $F(\kappa)$ is real-valued even if both k_j 's or one of these are imaginary. As expected, no bound states exist if $V_j \geq 0$ ($j = 1, 2$) because in this case $F(\kappa) > 0$ and the equation $F(\kappa) = 0$ has no solutions. The same situation takes place if one of V_j 's or both ones are negative, but satisfy the inequalities $\kappa^2 \geq |V_j|$, $j = 1, 2$. Therefore at least one of V_j 's has to be negative and then the interval of admissible non-zero values for κ is the interval $0 < \kappa < \max_{j=1,2} |V_j|^{1/2}$. In other words, the solutions of the equation $F(\kappa) = 0$ have to be analyzed for the two shapes of the potential profile (21): (i) one of the layers is of a barrier and the other one of a well form, and (ii) both the layers are of a well form.

Thus, solving the equation $F(\kappa) = 0$ with respect to $\tan(k_1 l_1)$ if $V_1 \leq V_2$ or $\tan(k_2 l_2)$ if $V_2 \leq V_1$ and replacing the variable κ by $\chi = k_1 l_1$ (if $V_1 \leq V_2$) and $\chi = k_2 l_2$ (if $V_2 \leq V_1$) via the relations

$$\kappa = \begin{cases} \sqrt{|V_1| - (\chi/l_1)^2} & \text{if } V_1 \leq V_2, \\ \sqrt{|V_2| - (\chi/l_2)^2} & \text{if } V_2 \leq V_1, \end{cases} \quad (65)$$

we arrive at the equation

$$\tan \chi = y(\chi), \quad y(\chi) := \frac{C_0}{\chi C_1 - \chi^{-1} C_2}, \quad (66)$$

having the same form in both the cases $V_1 \leq V_2$ and $V_2 \leq V_1$. Here

$$C_0 := 2 + \left(\frac{\sqrt{\rho^2 - \chi^2}}{\zeta} - \frac{\zeta}{\sqrt{\rho^2 - \chi^2}} \right) \tan \bar{\zeta}, \quad (67)$$

$$C_1 := \frac{1}{\sqrt{\rho^2 - \chi^2}} + \left(\frac{1}{\zeta} - \frac{\zeta}{\rho^2 - \chi^2} t_0 \right) \frac{\tan \bar{\zeta}}{1 + t_0}, \quad (68)$$

$$C_2 := \sqrt{\rho^2 - \chi^2} - \left(\zeta - \frac{\rho^2 - \chi^2}{\zeta} t_0 \right) \frac{\tan \bar{\zeta}}{1 + t_0}, \quad (69)$$

where

$$\chi = \begin{cases} k_1 l_1 = l_1 \sqrt{|V_1| - \kappa^2} & \text{if } V_1 \leq V_2 \quad (V_1 < 0), \\ k_2 l_2 = l_2 \sqrt{|V_2| - \kappa^2} & \text{if } V_2 \leq V_1 \quad (V_2 < 0). \end{cases} \quad (70)$$

The other parameters in equations (66)–(69) are given by

$$\zeta = \begin{cases} \zeta_1 := k_2 l_1 = [\chi^2 - \rho_1^2 - V_2 l_1^2]^{1/2} & \text{if } V_1 \leq V_2, \\ \zeta_2 := k_1 l_2 = [\chi^2 - \rho_2^2 - V_1 l_2^2]^{1/2} & \text{if } V_2 \leq V_1, \end{cases} \quad \bar{\zeta} = \begin{cases} \bar{\zeta}_1 := \zeta_1 l_2 / l_1, \\ \bar{\zeta}_2 := \zeta_2 l_1 / l_2, \end{cases} \quad (71)$$

$$\rho = \begin{cases} \rho_1 := |V_1|^{1/2} l_1 & \text{if } V_1 \leq V_2, \\ \rho_2 := |V_2|^{1/2} l_2 & \text{if } V_2 \leq V_1, \end{cases} \quad (72)$$

$$t_0 = \begin{cases} t_{0,1} := \tanh\left(\sqrt{\rho_1^2 - \chi^2} r/l_1\right) & \text{if } V_1 \leq V_2, \\ t_{0,2} := \tanh\left(\sqrt{\rho_2^2 - \chi^2} r/l_2\right) & \text{if } V_2 \leq V_1. \end{cases} \quad (73)$$

The roots of equation (66) are defined by the points of intersecting the function $y(\chi)$, defined on the interval $0 < \chi < \rho$, with the tan-function being ‘standing’ as ρ changes. In such a picture, it follows that the number of roots (say, N) is finite and this number depends on ρ . Let us arrange the roots in the order $\chi_1 > \chi_2 > \dots > \chi_N$ (numbered from the right to the left). Correspondingly, because of the relations

$$\kappa_i = l^{-1} \sqrt{\rho^2 - \chi_i^2}, \quad l := \begin{cases} l_1 & \text{if } V_1 \leq V_2, \\ l_2 & \text{if } V_2 \leq V_1, \end{cases} \quad i = 1, \dots, N, \quad (74)$$

following from equations (70), the levels κ_i ’s will be arranged in the order $\kappa_1 < \kappa_2 < \dots < \kappa_N$.

Consider first the situation when one of the layers is a barrier. Then, according to definition (71), we have

$$\zeta = iw = i \begin{cases} w_1 := \sqrt{\rho_1^2 - \chi^2 + V_2 l_1^2}, \\ w_2 := \sqrt{\rho_2^2 - \chi^2 + V_1 l_2^2}, \end{cases} \quad \tan \bar{\zeta} = i \begin{cases} \tanh(w_1 l_2 / l_1), \\ \tanh(w_2 l_1 / l_2), \end{cases} \quad (75)$$

and, as a result, the terms C_0 , C_1 and C_2 in equations (67)–(69) are positive functions of χ on the whole interval $0 < \chi < \rho$. Therefore, in the neighbourhood of the origin $\chi = 0$, the function $y(\chi)$ is negative (see figure 1), where $\lim_{\chi \rightarrow 0} y(\chi) = 0$. At the other

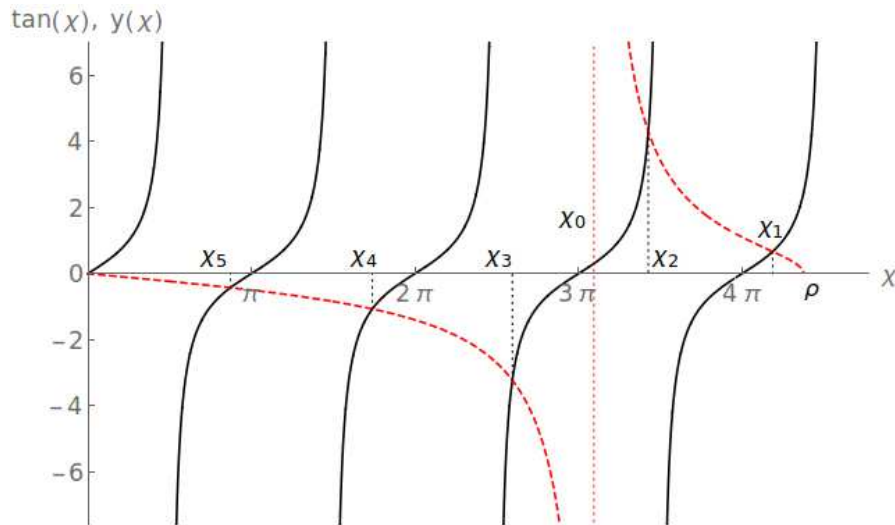


Figure 1. Graphical solution of equation (66), where the functions $\tan \chi$ and $y(\chi)$ are shown by solid (black) and dashed (red) curves, respectively. Five roots χ_1, \dots, χ_5 have been obtained as a result of intersecting these functions. Here $\rho = 13.7$ and the function $y(\chi)$ has one infinite discontinuity at point $\chi = \chi_0$.

end $\chi = \rho$, as follows from equations (68) and (69), we have $C_1 \rightarrow +\infty$ and $C_2 \rightarrow \text{const.}$ Then from equation (66) one can conclude that in the vicinity of the point $\chi = \rho$, the function $y(\chi)$ is positive. Since $C_0 > 0$ on the whole interval $(0, \rho)$ and the signs of the function $y(\chi)$ in the vicinity of the ends $\chi = 0$ and $\chi = \rho$ are opposite, the denominator of $y(\chi)$ has one zero. Therefore the function $y(\chi)$ has an infinite discontinuity at the point $\chi_0 = \rho/\sqrt{2}$ as shown in figure 1. On the interval $(0, \chi_0)$, the function $y(\chi)$ is negative and positive on the interval (χ_0, ρ) .

For the double-well (DW) form of potential (21), some additional points of infinite discontinuity can appear and they will be located to the right of the point χ_0 . This follows from equations (71) because at the point $\chi = l_1\sqrt{V_2 - V_1}$ (if $V_1 \leq V_2$) or $\chi = l_2\sqrt{V_1 - V_2}$ (if $V_2 \leq V_1$), the parameter ζ changes from imaginary to real values. Therefore the points of infinite discontinuity can appear on the intervals $l_1\sqrt{V_2 - V_1} < \chi < \rho_1$ (if $V_1 \leq V_2$) or $l_2\sqrt{V_1 - V_2} < \chi < \rho_2$ (if $V_2 \leq V_1$). In the limit as ρ approaches the origin, the function $y(\chi)$ is negative on some interval $0 < \chi < \chi_0$, where χ_0 is the point of the first infinite discontinuity that also approaches the origin as $\rho \rightarrow 0$. Therefore for sufficiently small ρ , only one root of equation (66) survives and it will be located on the interval $(0, \pi/2)$. Hence equation (66) can admit in the $\rho \rightarrow 0$ limit only one root.

Note that during the realization of point interactions in the squeezing limit, the inequality $V_1(l_1) \leq V_2(l_2)$ [or $V_2(l_2) \leq V_1(l_1)$] must be retained, independently on l_1 and l_2 , because the parameter ζ in equations (66)–(69) must be either real or imaginary during the whole squeezing procedure. Indeed, this is true because in definition (71) for the DW case we have $\chi^2 - \rho_1^2 - V_2 l_1^2 = \chi^2 - (V_1 - V_2)l_1^2$ and similarly $\chi^2 - \rho_2^2 - V_1 l_2^2 = \chi^2 + (V_1 - V_2)l_2^2$, so that the sign of the difference $V_1 - V_2$ is preserved during the whole squeezing process.

Thus, for a finite double-layer structure, there exists a finite number N of solutions χ_1, \dots, χ_N to equation (66) as illustrated by figure 1. In the limit as $\rho \rightarrow 0$, only the root χ_N survives. However, in spite of the existence of this root that approaches $\rho \rightarrow 0$, a non-trivial limit of the level κ_N , which could follow from the N th equation (74), in general does not exist. Similarly, in the other limit as $\rho \rightarrow \text{const.} \neq 0$, it follows from equations (74) that only the root χ_1 can survive if it approaches ρ . Therefore in both these cases, $\sqrt{\rho^2 - \chi^2} \rightarrow 0$. Taking for account this behaviour, equations (66)–(69) can asymptotically be replaced by

$$\frac{\chi \tan \chi + \zeta \tan \bar{\zeta}}{\sqrt{\rho^2 - \chi^2}} \simeq 2 - \left(\frac{\chi}{\zeta} + \frac{\zeta}{\chi} - \frac{\chi \zeta r}{l\sqrt{\rho^2 - \chi^2}} \right) \tan \chi \tan \bar{\zeta}. \quad (76)$$

Because of the denominator, the left-hand side of this equation diverges as $\chi \rightarrow \rho$ and therefore we must impose the condition

$$\chi \tan \chi + \zeta \tan \bar{\zeta} = 0. \quad (77)$$

This is the necessary condition for the equation (76) to be well-defined in the limit as $\chi \rightarrow \rho$. Coming back, according to equations (70)–(72), to the variables $k_j l_j$, $j = 1, 2$, one immediately finds that equation (77) reduces to resonance sets (57). The last term

in the right-hand side of equation (76) may be finite as $\chi \rightarrow \rho$ if $r \rightarrow 0$ sufficiently fast. Setting additionally $l\sqrt{\rho^2 - \chi_N^2} = \kappa_N$ if $\rho \rightarrow 0$ and $l\sqrt{\rho^2 - \chi_1^2} = \kappa_1$ if $\rho \rightarrow \text{const.} \neq 0$, we get from equation (76) the same asymptotic representation $\kappa_i \simeq \Delta/(z_1 + z_2)$ with $i = 1$ or N , where Δ , z_1 and z_2 are defined by equations (49) and (50). Therefore, *only* on resonance sets (57), κ_1 or κ_N converges to the bound state level κ defined by equations (63). In summary, we conclude that the convergence of the multiple bound states $\kappa_1, \dots, \kappa_N$ to a single level κ proceeds in the two ways: (i) in the case if $\rho \rightarrow 0$, the lowest energy level $\kappa_N \rightarrow \kappa$, whereas the rest of higher levels tend to zero, i.e.,

$$\kappa_1 \rightarrow 0, \kappa_2 \rightarrow 0, \dots, \kappa_{N-1} \rightarrow 0, \quad \kappa_N \rightarrow \kappa > 0, \quad (78)$$

(ii) contrary, in the case if $\rho \rightarrow \text{const.} \neq 0$, the highest energy level $\kappa_1 \rightarrow \kappa$, while the rest lower levels escape to infinity, resulting in the convergence sequence

$$\kappa_1 \rightarrow \kappa > 0, \quad \kappa_2, \dots, \kappa_N \rightarrow \infty. \quad (79)$$

6. Three-scale power-connecting parametrization of a double-layer potential

Thus, for realizing both separated and non-separated point interactions from a double-layer structure, the layer widths l_1 , l_2 and the distance between the layers r in potential (21) are required to shrink to the origin $x = 0$ along any path $\gamma = \{l_1, l_2, r\} \in \Gamma$. The Γ -space is interpreted as a pencil of paths that approach the origin obeying the limit conditions for the expressions listed in (29) and (30). Only on those paths belonging to the pencil Γ that form the resonance X - and Y -sets defined by equations (45) and (57), the non-separated point interactions are materialized, while beyond these sets the interactions are separated fulfilling boundary conditions (31). Moreover, on the resonance sets, the scattering data $a(k)$ and $b(k)$ as well as bound states are shown to exist as well-defined quantities. From a visualization point of view, in order to demonstrate the convergence of the discrete spectrum and the behaviour of the wave function in a squeezed limit, it would be convenient to parametrize the paths γ 's via an appropriately chosen *one* squeezing parameter, which could connect all the potential parameters V_1 , V_2 , l_1 , l_2 and r . There are various possible parametrizations of these parameters, each of which being a subset of the Γ -space. To this end, we choose here a power-connecting parametrization used in [54, 61, 62] for other purposes. It couples three positive powers μ , ν and τ via a dimensionless squeezing parameter $\varepsilon > 0$ as follows

$$V_1 = \varepsilon^{-\mu} h_1, \quad V_2 = \varepsilon^{-\nu} h_2, \quad l_1 = \varepsilon d_1, \quad l_2 = \varepsilon^{1-\mu+\nu} d_2, \quad r = \varepsilon^\tau c. \quad (80)$$

Here the coefficients $h_j \in \mathbb{R}$, $j = 1, 2$, are characteristic quantities of the system, so that they may be called the layer intensities (or amplitudes). In the following, we denote potential (21) parametrized by equations (80) as $V_\varepsilon(x)$. Clearly, the dependence of V_1 and V_2 on l_1 and l_2 can be expressed from (80) explicitly using a power gymnastics. Then, for the limits $|V_j(l_j)|^{1/2} l_j \rightarrow c_j \geq 0$, $j = 1, 2$, to be fulfilled, the conditions on the parameters μ and ν can be found and they will be given below.

6.1. Existence set for the distribution $\delta'(x)$

The explicit representation (80) allows us to define in the $\{\mu, \nu, \tau\}$ -space the set where potential (21) converges to $\delta'(x)$ in the sense of distributions. Thus, using the fast variable $\xi = x/\varepsilon$, for any test function $\varphi(x) \in C_0^\infty(\mathbb{R})$, we have

$$\begin{aligned} \langle V_\varepsilon(x) | \varphi(x) \rangle &= \int_0^{l_1+l_2+r} V_\varepsilon(x) \varphi(x) dx \\ &= \varepsilon \left[h_1 \varepsilon^{-\mu} \int_0^{d_1} \varphi(\varepsilon \xi) d\xi + h_2 \varepsilon^{-\nu} \int_{d_1+c\varepsilon^{\tau-1}}^{d_1+d_2\varepsilon^{\nu-\mu}+c\varepsilon^{\tau-1}} \varphi(\varepsilon \xi) d\xi \right]. \end{aligned} \quad (81)$$

Expanding next $\varphi(\varepsilon \xi) = \varphi(0) + \varepsilon \xi \varphi'(0) + (\varepsilon \xi)^2 \varphi''(0)/2 + \mathcal{O}(\varepsilon^3)$, we compute

$$\begin{aligned} \langle V_\varepsilon(x) | \varphi(x) \rangle &= \varepsilon^{1-\mu} (h_1 d_1 + h_2 d_2) \varphi(0) + \frac{\varepsilon^{2-\mu}}{2} [h_1 d_1^2 + \varepsilon^{\nu-\mu} h_2 d_2^2 \\ &\quad + 2h_2 d_2 (d_1 + \varepsilon^{\tau-1} c)] \varphi'(0) + \mathcal{O}(\varepsilon^{3-\mu}) + \mathcal{O}(\varepsilon^{3-3\mu+2\nu}) \\ &\quad + \mathcal{O}(\varepsilon^{\tau+2-\mu+\nu}) + \mathcal{O}(\varepsilon^{\tau+2-2\mu+2\nu}) + \mathcal{O}(\varepsilon^{2\tau+1-\mu+\nu}). \end{aligned} \quad (82)$$

The first term in this expansion diverges if $\mu > 1$. However, it cancels out under the condition

$$h_1 d_1 + h_2 d_2 = 0 \quad (83)$$

as a necessary condition for the existence of $\delta'(x)$. It can be fulfilled only either on the second (WB structure) or on the fourth (BW structure) quadrant of the $\{h_1, h_2\}$ -plane at given widths d_1 and d_2 . For the analysis of the second term in expansion (82), in the $\{\mu, \nu, \tau\}$ -space we single out the trihedral angle formed by vertex P_1 , edges K_1, L_1, N_1 and planes Q_1, O_1, S_1 , with interior space set I_1 , which are defined by the equations

$$\begin{aligned} P_1 &:= \{\mu = \nu = 2, \tau = 1\}, \\ K_1 &:= \{1 < \mu < 2, \nu = 2(\mu - 1), \tau = \mu - 1\}, \\ L_1 &:= \{\mu = 2, 2 < \nu < \infty, \tau = 1\}, \\ N_1 &:= \{\mu = \nu = 2, 1 < \tau < \infty\}, \\ Q_1 &:= \{1 < \mu < 2, \nu = 2(\mu - 1), \mu - 1 < \tau < \infty\}, \\ O_1 &:= \{\mu = 2, 2 < \nu < \infty, 1 < \tau < \infty\}, \\ S_1 &:= \{1 < \mu < 2, 2(\mu - 1) < \nu < \infty, \tau = \mu - 1\}, \\ I_1 &:= \{1 < \mu < 2, 2(\mu - 1) < \nu < \infty, \mu - 1 < \tau < \infty\} \end{aligned} \quad (84)$$

and illustrated by figure 2. In the set I_1 , the second term in expansion (82) vanishes as $\varepsilon \rightarrow 0$, whereas beyond the angle it diverges in this limit. It is remarkable that on the angle surface $S_{\delta'} := P_1 \cup K_1 \cup L_1 \cup N_1 \cup Q_1 \cup O_1 \cup S_1$ the second term has finite limit values. The remainder terms in expansion (82) tend to zero in the limit as $\varepsilon \rightarrow 0$ because all the powers therein are positive if they are considered on the surface $S_{\delta'}$. Therefore, with taking for account equation (83), we have

$$\langle V_\varepsilon(x) | \varphi(x) \rangle \simeq -\frac{h_1 d_1}{2} \varepsilon^{2-\mu} (d_1 + \varepsilon^{\nu-\mu} d_2 + 2\varepsilon^{\tau-1} c) \varphi'(0). \quad (85)$$

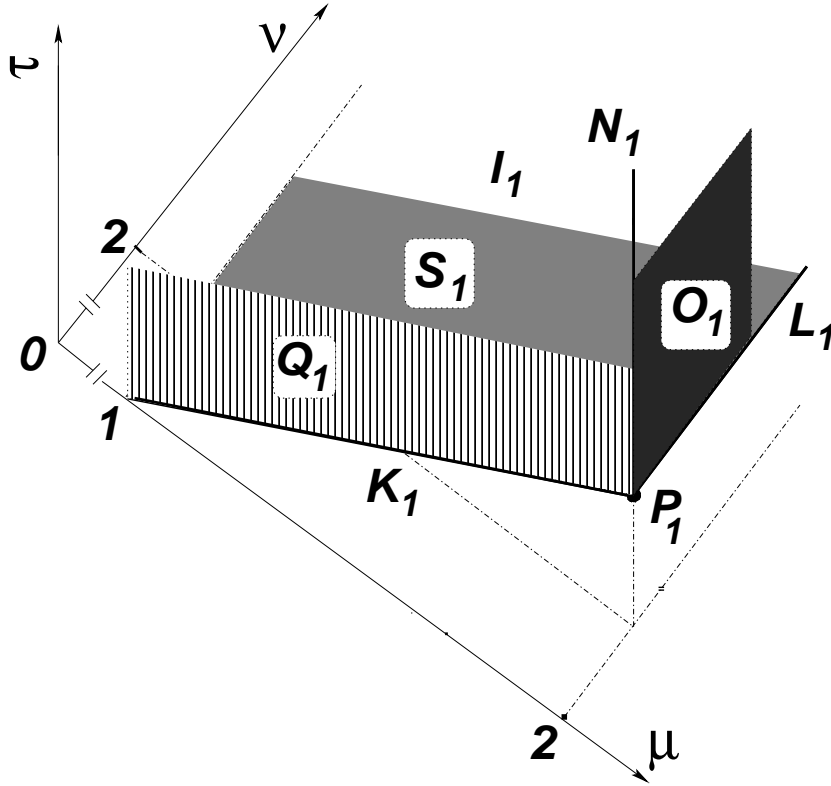


Figure 2. The S_γ -surface of the existence of the distribution $\delta'(x)$ obtained from a double-layer structure. The elements of this surface are defined by equations (84).

It follows from this asymptotic representation that the potential $V_\varepsilon(x)$ converges to $\gamma\delta'(x)$ in the sense of distributions if condition (83) holds true. Here, the strength constant γ is the set function defined by

$$\gamma = \frac{h_1 d_1}{2} \begin{cases} d_1 + d_2 + 2c & \text{at point } P_1, \\ d_2 + 2c & \text{on line } K_1, \\ d_1 + 2c & \text{on line } L_1, \\ d_1 + d_2 & \text{on line } N_1, \\ d_2 & \text{on area } Q_1, \\ d_1 & \text{on area } O_1, \\ 2c & \text{on area } S_1. \end{cases} \quad (86)$$

Thus, under condition (83), the surface S_γ separates in the $\{\mu, \nu, \tau\}$ -space the volume region I_1 of perfect transmission and the region of non-existence of point interactions.

6.2. Parametrized resonance sets and scattering data

The three-scale parametrization given by equations (80) allows us to realize the geometric diagram in the $\{\mu, \nu, \tau\}$ -space (depicted in figure 3), where the sets for all the four cases of the $\varepsilon \rightarrow 0$ limits of the arguments $k_1 l_1$ and $k_2 l_2$, i.e., (i) $k_1 l_1 \rightarrow \sigma_1 \neq 0$ and $k_2 l_2 \rightarrow \sigma_2 \neq 0$, (ii) $k_1 l_1 \rightarrow 0$ and $k_2 l_2 \rightarrow \sigma_2 \neq 0$, (iii) $k_1 l_1 \rightarrow \sigma_1 \neq 0$ and $k_2 l_2 \rightarrow 0$, (iv)

$k_1 l_1 \rightarrow 0$ and $k_2 l_2 \rightarrow 0$, can be represented. The $\varepsilon \rightarrow 0$ limits of $k_j l_j$'s, $j = 1, 2$, define the four sets on the $\{\mu, \nu\}$ -plane section, on which

$$k_1 l_1 \simeq \varepsilon^{1-\mu/2} \sqrt{-h_1} d_1 \quad \text{and} \quad k_2 l_2 \simeq \varepsilon^{1-\mu+\nu/2} \sqrt{-h_2} d_2. \quad (87)$$

The other eight limits $f_j, \eta_j, g_j, \beta_j$ ($j = 1, 2$) defined by equations (44) and (56) determine the power τ as a function of μ and ν . Their asymptotic representation is

$$\begin{aligned} f_1 &\simeq k_1 r \simeq \varepsilon^{\tau-\mu/2} \sqrt{-h_1} c, & f_2 &\simeq k_2 r \simeq \varepsilon^{\tau-\nu/2} \sqrt{-h_2} c, \\ \eta_j &\simeq k_j^2 l_j r \simeq -\varepsilon^{\tau-\mu+1} h_j d_j c \end{aligned} \quad (88)$$

for the resonance sets $X = \{X_{11}, X_{01}, X_{10}, X_{00}\}$ and

$$\begin{aligned} g_1 &\simeq k_1 r^{1/2} \simeq \varepsilon^{(\tau-\mu)/2} \sqrt{-h_1} c, & g_2 &\simeq k_2 r^{1/2} \simeq \varepsilon^{(\tau-\nu)/2} \sqrt{-h_2} c, \\ \beta_j &\simeq k_j^2 l_j r^{1/2} \simeq -\varepsilon^{\tau/2-\mu+1} h_j d_j c^{1/2} \end{aligned} \quad (89)$$

for the resonance sets $Y = \{Y_{11}, Y_{01}, Y_{10}, Y_{00}\}$. Hence asymptotic representation (87)–(89) admits either finite limits

$$\begin{aligned} \sigma_j &= \sqrt{-h_j} d_j, & f_j &= \sqrt{-h_j} c, & \eta_j &= -h_j d_j c & \text{for } X\text{-sets,} \\ \sigma_j &= \sqrt{-h_j} d_j, & g_j &= \sqrt{-h_j} c, & \beta_j &= -h_j d_j c^{1/2} & \text{for } Y\text{-sets,} \end{aligned} \quad (90)$$

or zero. Therefore equations (45) together with relations (90) for X -sets are reduced to

$$\left. \begin{aligned} X_{11} &: \cot(\sqrt{-h_1} d_1) / \sqrt{-h_1} + \cot(\sqrt{-h_2} d_2) / \sqrt{-h_2} \\ X_{01} &: -1/h_1 d_1 + \cot(\sqrt{-h_2} d_2) / \sqrt{-h_2} \\ X_{10} &: \cot(\sqrt{-h_1} d_1) / \sqrt{-h_1} - 1/h_2 d_2 \\ X_{00} &: -1/h_1 d_1 - 1/h_2 d_2 \end{aligned} \right\} = c \quad \begin{array}{l} \text{at } P_1, \\ \text{on } K_1, \\ \text{on } L_1, \\ \text{on } S_1. \end{array} \quad (91)$$

Inserting next values (90) into equations (46), we get the element θ and consequently the scattering data a and b given by equations (47) that do not depend on k .

Similarly, inserting values (90) for Y -sets into equations (57), we obtain the explicit representation of the resonance sets:

$$\left. \begin{aligned} Y_{11} &: \sqrt{-h_1} \tan(\sqrt{-h_1} d_1) + \sqrt{-h_2} \tan(\sqrt{-h_2} d_2) \\ Y_{01} &: h_1 d_1 - \sqrt{-h_2} \tan(\sqrt{-h_2} d_2) \\ Y_{10} &: \sqrt{-h_1} \tan(\sqrt{-h_1} d_1) - h_2 d_2 \\ Y_{00} &: h_1 d_1 + h_2 d_2 \end{aligned} \right\} = 0 \quad \text{on} \quad \left\{ \begin{array}{l} P_2 \cup N_2, \\ K_2 \cup Q_2, \\ L_2 \cup O_2, \\ S_2 \cup I_2, \end{array} \right. \quad (92)$$

where the sets

$$\begin{aligned} P_2 &:= \{\mu = \nu = \tau = 2\}, \\ K_2 &:= \{1 < \mu < 2, \nu = \tau = 2(\mu - 1)\}, \\ L_2 &:= \{\mu = 2, 2 < \nu < \infty, \tau = 2\}, \\ N_2 &:= \{\mu = \nu = 2, 2 < \tau < \infty\}, \\ Q_2 &:= \{1 < \mu < 2, \nu = 2(\mu - 1), \mu - 1 < \tau < \infty\}, \\ O_2 &:= \{\mu = 2, 2 < \nu < \infty, 2 < \tau < \infty\}, \\ S_2 &:= \{1 < \mu < 2, 2(\mu - 1) < \nu < \infty, \tau = 2(\mu - 1)\}, \\ I_2 &:= \{1 < \mu < 2, 2(\mu - 1) < \nu < \infty, 2(\mu - 1) < \tau < \infty\} \end{aligned} \quad (93)$$

form the second trihedral angle with vertex P_2 , edges K_2, L_2, N_2 and planes Q_2, O_2, S_2 , including interior space set I_2 (see figure 3). Inserting now values (90) for the Y -sets into

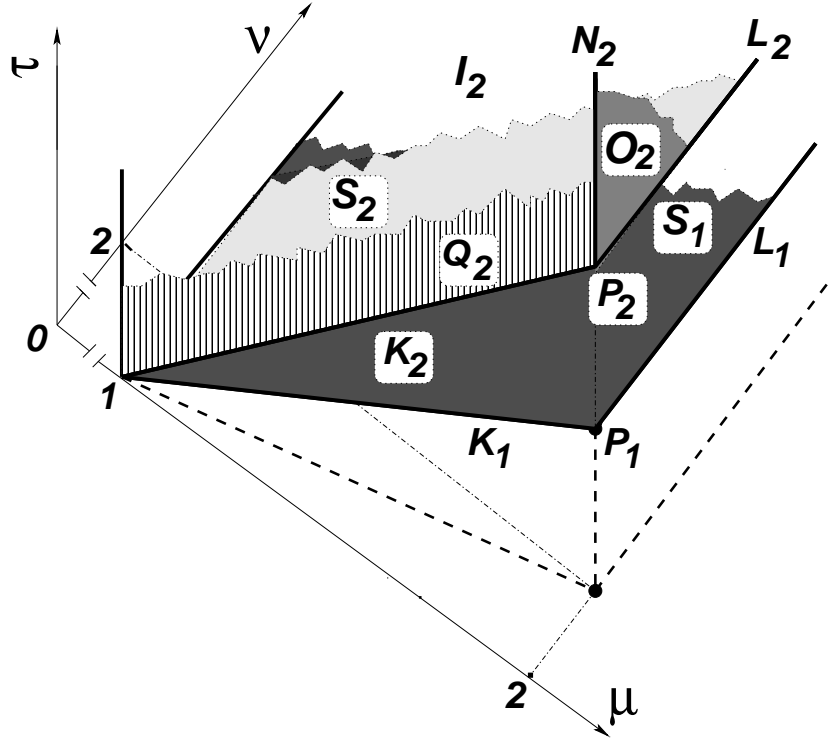


Figure 3. Sets defined by equations (84) and (93) on which the point interactions of the first (with subscript ‘1’) and the second (with subscript ‘2’) types are realized. The sets of the first type are found on the plane $\{1 < \mu \leq 2, 2(\mu - 1) \leq \nu < \infty, \tau = \mu - 1\}$, whereas the interactions of the second type in the space $\{1 < \mu \leq 2, 2(\mu - 1) \leq \nu < \infty, 2(\mu - 1) \leq \tau < \infty\}$.

equations (58) and (59), we obtain the expressions for the elements θ and α which make sense only in the second trihedral angle on the resonance Y -sets, being the solutions to equations (92). Note that these solutions (the resonance Y_{11^-} , Y_{01^-} , Y_{10} -surfaces and Y_{00} -plane) appear to be the limits of the corresponding X -surfaces as formally $c \rightarrow 0$ [compare equations (91) and (92)].

According to asymptotic representation (89) with limit values (90) for the Y -sets, the elements θ given by the first formulas (58) and α defined by equations (59) are reduced to

$$\theta = \begin{cases} \cos(\sqrt{-h_1} d_1) / \cos(\sqrt{-h_2} d_2) \\ 1 / \cos(\sqrt{-h_2} d_2) \\ \cos(\sqrt{-h_1} d_1) \\ 1 \end{cases} \quad \text{on} \quad \begin{cases} P_2 \cup N_2, \\ K_2 \cup Q_2, \\ L_2 \cup O_2, \\ S_2 \cup I_2, \end{cases} \quad (94)$$

$$\alpha = h_1 h_2 c \begin{cases} (1 / \sqrt{-h_1} \sqrt{-h_2}) \sin(\sqrt{-h_1} d_1) \sin(\sqrt{-h_2} d_2) & \text{at } P_2, \\ (d_1 / \sqrt{-h_2}) \sin(\sqrt{-h_2} d_2) & \text{on } K_2, \\ (d_2 / \sqrt{-h_1}) \sin(\sqrt{-h_1} d_1) & \text{on } L_2, \\ d_1 d_2 & \text{on } S_2 \end{cases} \quad (95)$$

and $\alpha = 0$ in the space region $Q_2 \cup O_2 \cup N_2 \cup I_2$.

Thus, equations (91) and (92) are the conditions at which the scattering data $a(k)$ and $b(k)$ are well-defined quantities. At fixed d_1 and d_2 , the solutions of these equations can be represented on the $\{h_1, h_2\}$ -plane (more precisely, on the WB, DW and BW quadrants) in the form of curves, similarly to those depicted in the corresponding figures of work [54] (see figure 2 for X_{00} , and Y_{00} , figure 3 for X_{01} , and Y_{01} , figure 4 for X_{10} and Y_{10} , figure 5 for X_{11} and Y_{11} therein). The cancellation of divergences of the first type results in the existence of resonance X -sets (91) in the section plane $\tau = \mu - 1$, whereas the cancellation of the second type leads to the existence of resonance Y -sets in the space region $\tau \geq 2(\mu - 1)$.

From the whole family of point interactions, which are realized on the resonance sets described by equations (91) and (92), one can single out the interactions with additional condition (83) for the existence of the distribution $\delta'(x)$. Therefore the whole family realized in general from both the BW and DW configurations of potential (21) can be referred to as *generalized δ' -potentials*, while the subfamily restricted by constraint (83) *distributional* ones. The name ' δ' -potentials' (both generalized and distributional) comes from the fact that the element $\theta(k)$ determined by equations (46) and (58) on the X - and Y -sets except for the set Y_{00} does not identically equal the unity [14]. The point interaction with $\theta(k) = 1$ [see the last equations in (58) and (94)] may be called a *generalized δ -potential* because the corresponding profile of potential (21) has no a $\delta(x)$ limit as $\varepsilon \rightarrow 0$.

6.3. Bound state level κ

Inserting expressions (94) and (95) into the formula for the level κ in (62), on resonance sets (92), the level κ is

$$\begin{aligned}
 \kappa|_{P_2 \times Y_{11}} &= - \frac{h_1 c \tan^2(\sqrt{-h_1} d_1)}{\cos^{-2}(\sqrt{-h_1} d_1) + \cos^{-2}(\sqrt{-h_2} d_2)} \\
 &= - \frac{h_2 c \tan^2(\sqrt{-h_2} d_2)}{\cos^{-2}(\sqrt{-h_1} d_1) + \cos^{-2}(\sqrt{-h_2} d_2)}, \\
 \kappa|_{K_2 \times Y_{01}} &= \frac{(h_1 d_1)^2 c}{1 + \cos^{-2}(\sqrt{-h_2} d_2)} = \frac{h_2 c}{2(h_1 d_1)^{-2} h_2 - 1}, \\
 \kappa|_{L_2 \times Y_{10}} &= \frac{(h_2 d_2)^2 c}{1 + \cos^{-2}(\sqrt{-h_1} d_1)} = \frac{h_1 c}{2(h_2 d_2)^{-2} h_1 - 1}, \\
 \kappa|_{S_2 \times Y_{00}} &= \frac{1}{2} (h_1 d_1)^2 c = \frac{1}{2} (h_2 d_2)^2 c. \tag{96}
 \end{aligned}$$

6.4. Convergence of multiple bound state levels to a squeezed single value

Parametrization (80) as a particular pathway of materializing point interactions from a double-layer system, allows us to control explicitly the behaviour of all the roots χ_1, \dots, χ_N as the solutions of equation (66) with (67)–(69), under the shrinking of the system to a point. Accordingly, due to relations (74), one can observe the behaviour of bound state levels $\kappa_1, \dots, \kappa_N$. In particular, one can establish which of the lateral levels

κ_1 or κ_N converges to a single level κ . Contrary to the case with a single rectangular well, here the convergence is available *only* on the resonance Y -sets defined by equations (92). This means that the finite limit values for the bound state κ can be obtained if the powers μ , ν and τ are found on the plane $\tau = 2(\mu - 1)$, i.e., on the set $P_2 \cup K_2 \cup L_2 \cup S_2$, on one side, and on the other side, the system parameters h_1 , d_1 , h_2 , d_2 must obey equations (92), while $c > 0$ may be arbitrary.

Equation (66) has been derived for the variable χ that corresponds to the well (in the BW case) or to the deepest well (in the DW case). Therefore there are two cases: $V_1 < 0$, $V_2 \in \mathbb{R}$, $V_1 \leq V_2$ and $V_1 \in \mathbb{R}$, $V_2 < 0$, $V_1 \geq V_2$. The parameters ρ as well as ζ , $\bar{\zeta}$ and t_0 defined by equations (71)–(73) and involved into equations (67)–(69) are given explicitly in terms of μ , ν , τ and ε as follows

$$\begin{aligned} \rho_1 &= \varepsilon^{1-\mu/2} |h_1|^{1/2} d_1, \\ \zeta_1 &= [\chi^2 - \rho_1^2 - \varepsilon^{2-\nu} h_2 d_1^2]^{1/2}, \\ \bar{\zeta}_1 &= [\varepsilon^{2(\nu-\mu)} (\chi^2 - \rho_1^2) (d_2/d_1)^2 - \varepsilon^{2(1-\mu)+\nu} h_2 d_2^2]^{1/2}, \\ t_{0,1} &= \tanh \left[\varepsilon^{\tau-1} (c/d_1) \sqrt{\rho_1^2 - \chi^2} \right] \end{aligned} \quad (97)$$

if $V_1 \leq V_2$ and

$$\begin{aligned} \rho_2 &= \varepsilon^{1-\mu+\nu/2} |h_2|^{1/2} d_2, \\ \zeta_2 &= [\chi^2 - \rho_2^2 - \varepsilon^{2-3\mu+2\nu} h_1 d_2^2]^{1/2}, \\ \bar{\zeta}_2 &= [\varepsilon^{2(\mu-\nu)} (\chi^2 - \rho_2^2) (d_1/d_2)^2 - \varepsilon^{2-\mu} h_1 d_1^2]^{1/2}, \\ t_{0,2} &= \tanh \left[\varepsilon^{\tau-1+\mu-\nu} (c/d_2) \sqrt{\rho_2^2 - \chi^2} \right] \end{aligned} \quad (98)$$

if $V_2 \leq V_1$. Note that one of the sets of equations (97) or (98) must be used during the squeezing procedure as $\varepsilon \rightarrow 0$, at least beginning from some small value $\varepsilon > 0$. Which of these sets has to be applied, depends on the shape of the potential $V_\varepsilon(x)$. The configurations (i), (ii) and (iii) listed below cover all the possible situations for the existence of bound states. (i) WB profile ($h_1 < 0$, $h_2 > 0$): any μ and ν , equations (97) to be used. (ii) BW profile ($h_1 > 0$, $h_2 < 0$): any μ and ν , equations (98) to be used. (iii) DW profile ($h_1 < 0$, $h_2 < 0$): $h_1 \leq h_2$ and $\mu = \nu$ or any h_1 , h_2 and $\mu > \nu$, equations (97) to be used; $h_1 \geq h_2$ and $\mu = \nu$ or any h_1 , h_2 and $\mu < \nu$, equations (98) to be used.

Equations (97) and (98) are used for the graphical illustration as the finite number of bound state levels κ_i 's converges to a single level κ given by analytic expressions (96). Plotting $\tan \chi$ and $y(\chi)$ as functions of χ on the interval $0 < \chi < \rho$, expressed by equations (66)–(69) in which the parameters ζ , $\bar{\zeta}$, ρ and t_0 are given by one of equations (97) or (98), one can find the roots χ_i 's located at the intersection of the functions $\tan \chi$ and $y(\chi)$ as shown in figure 1.

The parameter values for the numerical solution of equation (66) are chosen from the $\{h_1, d_1, h_2, d_2\}$ -space, which obey equations (92), and the parameter $c > 0$ is supposed arbitrary. The powers μ , ν and τ belong to the point P_2 , one of the lines K_2 or L_2 and the plane S_2 defined by equations (93) and shown in figure 3. Having solved equation (66) at a given $\varepsilon > 0$, then its solutions χ_1, \dots, χ_N are inserted into equations (74) and the convergence of the levels $\kappa_1, \dots, \kappa_N$ is examined as $\varepsilon \rightarrow 0$. Note that the $\varepsilon \rightarrow 0$

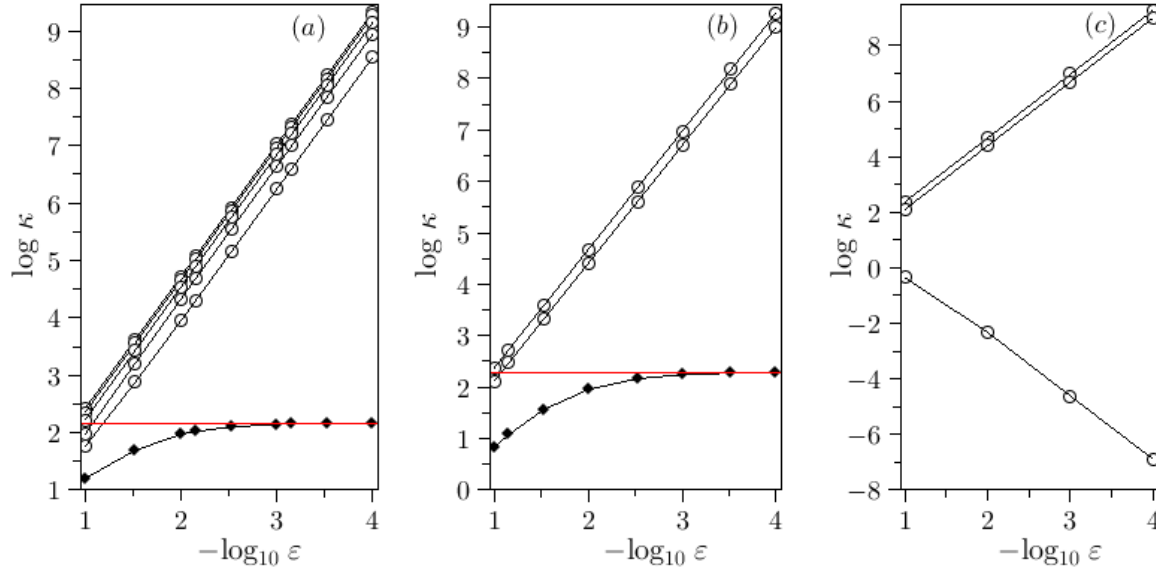


Figure 4. Convergence of bound state levels κ_i 's in the limit as $\varepsilon \rightarrow 0$ for the δ' -potentials realized from double-layer structure with parameters $h_2 = -0.5$ eV and $c = 20$ nm (for all cases below): (a) Generalized δ' -potential obtained from DW structure with parameters $h_1 = -0.3$ eV, $d_1 = 2.1$ nm and $d_2 = 12.0$ nm obeying the first equation (92) for P_2 . The $\{h_1, d_1, h_2, d_2\}$ -point with these parameter values lies on the 1st resonance surface of the Y_{11} -set. Figure 1 has been plotted for these values and the five levels $\kappa_1, \dots, \kappa_5$ as functions of ε correspond to the five roots χ_1, \dots, χ_5 at $\varepsilon = 1$. (b) Distributional δ' -potential materialized from BW structure with parameters $h_1 = 0.3$ eV, $d_1 = 10.1$ nm and $d_2 = 6.1$ nm fulfilling both the first equation (92) for P_2 and constraint (83). The $\{h_1, d_1, h_2, d_2\}$ -point with these parameter values lies on the intersection of the 2nd resonance surface of the Y_{11} -set and surface (83). For these values, there are three roots χ_1, χ_2, χ_3 at $\varepsilon = 1$. The solid (red) horizontal straight lines in (a) and (b) indicate the values for κ given by the formulas for $\kappa|_{P_2 \times Y_{11}}$ in (96). (c) Distributional δ' -potential obtained from BW profile with the same parameter values as in (b), but beyond the plane $\tau = 2(\mu - 1)$, lying on line N_2 with $\tau = 3$. Here, there are also three roots at $\varepsilon = 1$.

limit values of κ computed in this way must coincide with the analytic results given by equations (96). As follows from equations (97) and (98), in the limit as $\varepsilon \rightarrow 0$, either $\rho_j \rightarrow 0$ or $\rho_j \rightarrow |\sigma_j| = |h_j|^{1/2}d_j$, $j = 1, 2$. Below we describe the convergence of the levels κ_i 's on some sets of the $\{\mu, \nu, \tau\}$ -space and indicate which of equations (97) or (98) has to be used in each case.

Point P_2 : At this point the convergence of κ_i , $i = 1, \dots, N$, is of type (79). The generalized δ' -potentials are materialized from the WB, DW and BW configurations. Equations (97) are used if $h_1 \leq h_2 \in \mathbb{R}$ and equations (98) if $h_2 \leq h_1 \in \mathbb{R}$. The distributional δ' -potentials are realized on the WB and BW quadrants. The convergence of κ_i 's to the squeezed value κ obeying the first equation (96) is illustrated in figure 4: (a) for the generalized δ' -potential obtained from a DW profile and (b) for the distributional

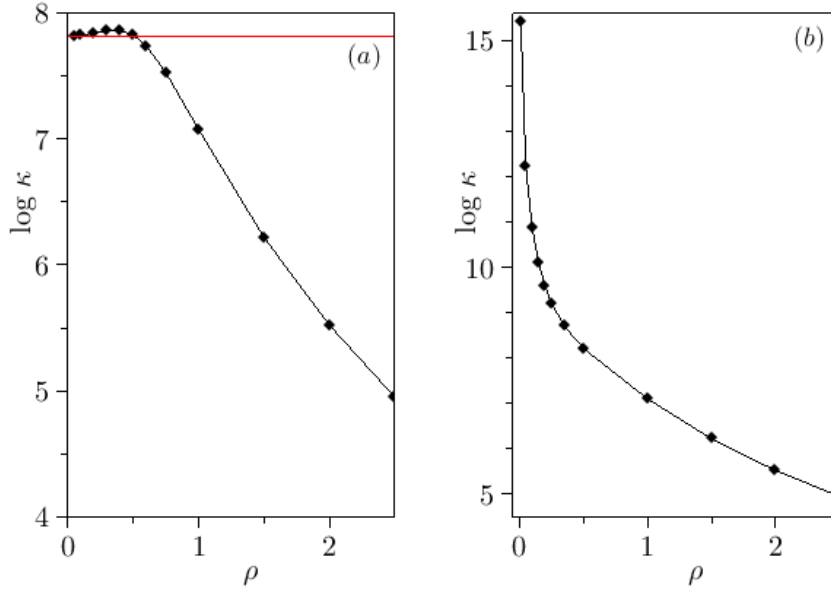


Figure 5. Convergence of the biggest (survived) bound state level κ_N as $\rho = \varepsilon^{1/4}|h_2|^{1/2}d_2 \rightarrow 0$ for point interactions realized from BW profile with parameters $h_1 = |h_2| = 0.5$ eV and $d_1 = d_2 = 12$ nm: (a) Generalized δ -potential obtained for the point $\{\mu = \nu = 3/2, \tau = 2(\mu - 1) = 1\}$ lying on plane S_2 . The solid (red) horizontal straight line indicates the value for κ given by the formulas for $\kappa|_{S_2 \times Y_{00}}$ in (96). (b) Point interaction of separated type (with full reflection) obtained for the same point on S_2 , but beyond the resonance condition $h_1 d_1 = |h_2| d_2 = 0$. Here, $d_1 = 8$ nm, $d_2 = 12$ nm and κ_N escapes to infinity.

δ' -potential realized from a BW profile.

Line N_2 : On this line located above the plane $\tau = 2(\mu - 1)$, the convergence of κ_i 's is also of type (79), except for the highest energy level κ_1 , which converges to zero. In figure 4(c), the convergence of this type is plotted for the distributional δ' -potential obtained from a BW profile.

Plane S_2 : On this plane the family of generalized δ -potentials can be materialized if the system parameters satisfy the last equation in (92), which coincides with condition (83) for the existence of the distribution $\delta'(x)$. Here the convergence is of type (78). The behaviour of κ_i 's is shown in figure 5(a) for the biggest level κ_N in the particular case: $\mu = \nu = 3/2$, $h_1 = -h_2$, $d_1 = d_2$, where $\rho = \varepsilon^{1/4}|h_2|^{1/2}d_2$. From equations (74) one finds the asymptotic behaviour of κ_N in the limit as $\rho \rightarrow 0$ (or $\varepsilon \rightarrow 0$) as follows

$$\kappa_N = \rho^{-4} \sqrt{\rho^2 - \chi_N^2} |h_2|^2 d_2^3. \quad (99)$$

Using here equations (76) and (77), one can arrive at the last formula (96). Beyond the resonance Y_{00} -set, we have that $\kappa_1 \rightarrow 0$, $\kappa_2 \rightarrow 0$, \dots , $\kappa_{N-1} \rightarrow 0$, but $\kappa_N \rightarrow \infty$ as shown in figure 5(b) for the level κ_N .

Line K_2 : On this line the family of generalized δ' -potentials can be realized from the WB, DW and BW profiles on the resonance Y_{01} -set defined by the second equation

(92). Equations (97) are used with $\rho_1 \rightarrow 0$ for the WB and DW (if $h_1 \leq h_2$ and $\mu = \nu$ or any h_1, h_2 and $\mu > \nu$) profiles. Equations (98) are used with $\rho_2 \rightarrow |h_2|^{1/2}d_2$ for the DW (if $h_1 \geq h_2$ and $\mu = \nu$ or any h_1, h_2 and $\mu < \nu$) and BW profiles. In the latter case, the distributional δ' -potentials are realized if condition (83) is imposed additionally. Here the convergence of type (79) takes place and the behaviour of κ_i 's is similar to that shown in figure 4(b).

Line L_2 : The situation on this line is similar to that as described for the line K_2 . Here the family of generalized δ' -potentials can also be realized from the WB, DW and BW profiles, but now on the resonance Y_{10} -set defined by the third equation (92). Equations (97) are used with $\rho_1 \rightarrow |h_1|^{1/2}d_1$ for the WB and DW (if $h_1 \leq h_2$ and $\mu = \nu$ or any h_1, h_2 and $\mu > \nu$) profiles. Equations (98) are used with $\rho_2 \rightarrow 0$ for the DW (if $h_1 \geq h_2$ and $\mu = \nu$ or any h_1, h_2 and $\mu < \nu$) and BW profiles. In the former case, when equations (97) have to be used, the distributional δ' -potentials are realized if condition (83) is imposed additionally. Here the convergence of type (79) takes place and the behaviour of κ_i 's is also similar to that shown in figure 4(b).

Thus, both generalized and distributional the δ' -potentials with non-zero bound states can be realized on the intersection of the plane $\tau = 2(\mu - 1)$ with the surface $S_{\delta'}$, i.e., at the point P_2 and on the lines K_2 and L_2 . The convergence of the levels κ_i 's for the point P_2 is of type (79), while on the lines K_2 and L_2 it can be of both types (78) and (79). Above these sets, on the line N_2 and on the planes Q_2 and O_2 , the situation is quite similar, but here $\kappa_N \rightarrow 0$ in sequence (78) and $\kappa_1 \rightarrow 0$ in sequence (79).

6.5. Convergence of wave functions in a squeezed limit

Parametrization (80) of potential (21) allows us to illustrate a pointwise convergence of solutions to equation (1) in the limit as $\varepsilon \rightarrow 0$, both for positive ($k^2 > 0$) and negative ($k^2 = -\kappa^2$) energies. For a non-separated point interaction to be realized, the system parameters h_1, h_2, d_1, d_2 must belong to one of the resonance X - or Y -sets described by equations (91) and (92). It is of interest to plot the wave functions on one of the Y -sets, because on these sets bound states are available. Therefore, as an appropriate example, we choose here a BW structure with the parameter values corresponding to the Y_{11} -set and determined by the first equation in (92).

Thus, on the basis of formula (32), the function $\phi_1(x)$ describing an incident plane wave (with a given k) from the right is plotted in figure 6 for three situations of shrinking a BW structure. The parameter values h_1, h_2, d_1, d_2 satisfy the first equation in (92). For these values and the same three scales of squeezing the BW structure, the function $\phi_1(x)$, which describes a bound state, is plotted in figure 7 using the same equations (32) with $k = i\kappa$. The panels (c) in both figures clearly illustrate the appearance of a jump at $x = 0$ that agrees with the first equation in (61), where θ is computed from the first equation in (94).

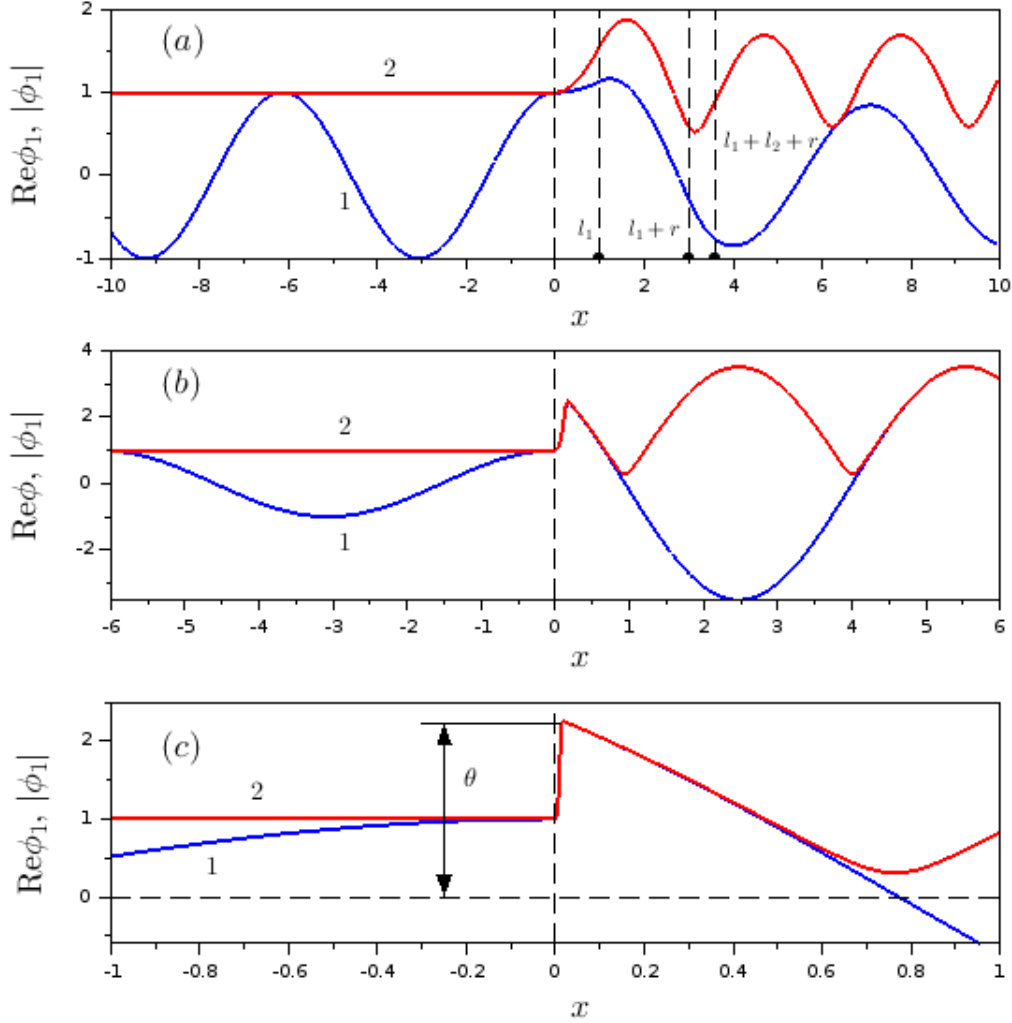


Figure 6. Profiles $\text{Re}\phi_1(x)$ (blue curves, 1) and $|\phi_1(x)|$ (red curves, 2) for (a) $\varepsilon = 1$, (b) $\varepsilon = 0.1$, (c) $\varepsilon = 0.01$. The system parameter values are $h_1 = 0.5$ eV, $h_2 = -0.5$ eV, $d_1 = 1.0$ nm, $d_2 = 0.6$ nm and $c = 2.0$ nm. The energy of an incident particle is $k^2 = 0.4$ eV. In the squeezing limit [panel (c)], the jump of function $\phi_1(x)$ at $x = 0$ reaches the value $\theta - 1$ with $\theta = 2.23$.

7. Concluding remarks

The procedure of squeezing a double-layer structure developed in this article is based on the simultaneous shrinking of the system parameters l_1 , l_2 and r to zero, which can be arranged in different ways. In this regard, the two families of the strength functions $V_1(l_1)$ and $V_2(l_2)$ have been defined by limit equations (43)–(44) and (55)–(56). These equations are expressed in terms of the limit characteristics $\sigma_j = \lim_{l_j \rightarrow 0} (k_j l_j)$, $j = 1, 2$. The other eight limit characteristics involve the dependence on distance r : $f_j, \eta_j \sim r^{-1}$ and $g_j, \beta_j \sim r^{-1/2}$.

The squeezed limit of the scattering functions $a(k)$ and $b(k)$ is proven to be well-defined only if some constraints on the limit characteristics are imposed. These

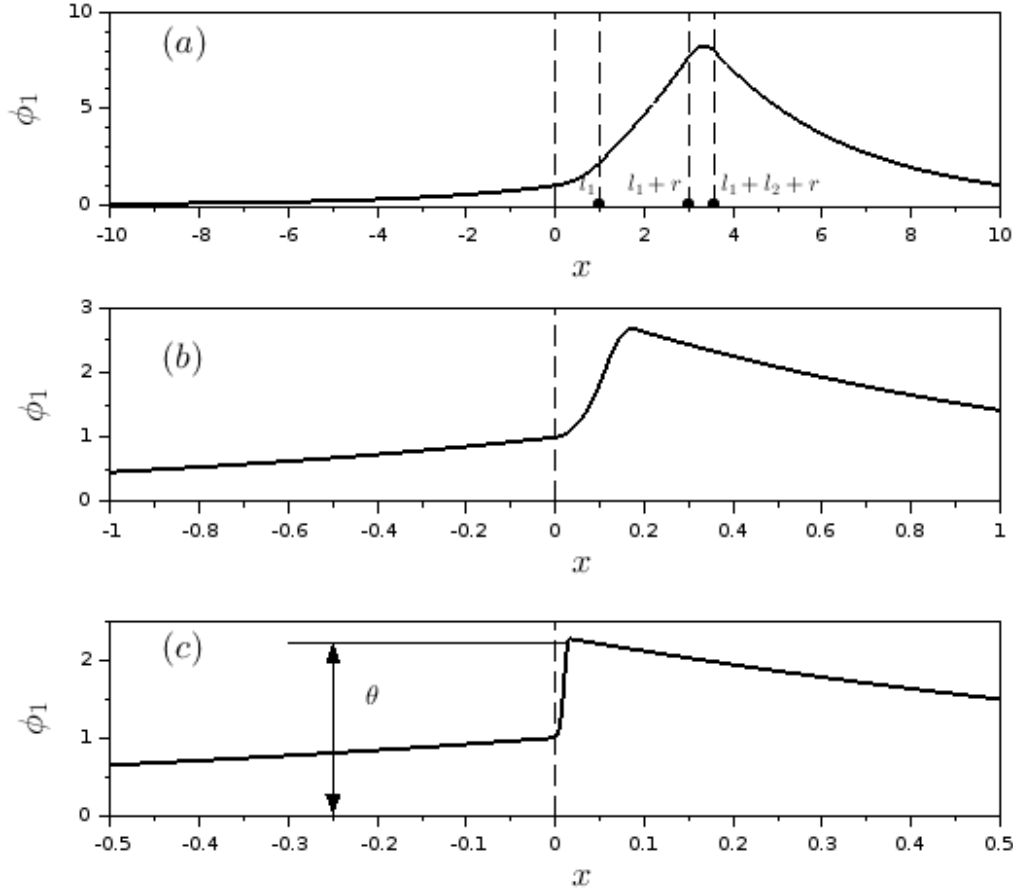


Figure 7. Eigenfunction $\phi_1(x)$ plotted for (a) $\varepsilon = 1$, (b) $\varepsilon = 0.1$, (c) $\varepsilon = 0.01$. The system parameter values and θ are the same as in figure 6. Here the bound state levels are $\kappa = 0.320$ ($\varepsilon = 1$), $\kappa = 0.773$ ($\varepsilon = 0.1$), $\kappa = 0.864$ ($\varepsilon = 0.01$). The jump at $x = 0$ illustrated by panel (c) is the same as in figure 6(c).

constraints are referred to as resonance sets, resulting from the two ways of the cancellation of divergences in the singular function $\Delta(k)$ given by formula (36). The first way is to put $\Delta(k) = 0$, leading to the derivation of the resonance X -sets defined by equations (45). The second way requires that the squeezed limit of the function $\Delta(k)$ is a non-zero constant, In this way, the resonance Y -sets are defined by equations (57), on which the point interactions with non-trivial bound states can be realized.

As a particular example of the whole variety of the shrinking ways, we have chosen the three-scale parametrization [see equations (80)], where all the system parameters are connected through a dimensionless squeezing parameter $\varepsilon > 0$. This connection, used in earlier publications [54, 61, 62], allows us to construct the geometric representation in the three-dimensional space of positive powers μ , ν and τ .

The three-scale power-connecting parametrization allows us to single out in the $\{\mu, \nu, \tau\}$ -space the surface $S_{\delta'}$ of the existence of the distribution $\delta'(x)$ if condition (83) is imposed. This condition means that only barrier-well configurations are appropriate for the existence of $\delta'(x)$. On the other hand, except for these configurations, double-

well ones also participate in realizing the point interactions for which $a(k)$ and $b(k)$ are well-defined functions. In this article they are called generalized δ' -potentials.

There exists an ubiquitous opinion that the bound state energy levels for the Schrödinger equation (1) with a regularized potential $V_\varepsilon(x)$ escape to $-\infty$ as $V_\varepsilon(x) \rightarrow \beta\delta'(x)$ in the sense of distributions (β is a strength constant). In this article, it is shown that in general this is not true, except for the point interactions with an additional δ -like potential [13, 31, 32, 60, 62, 63, 64, 65], where $V(x) = \alpha\delta(x) + \beta\delta'(x)$, $\alpha < 0$, $\beta \in \mathbb{R}$. On the basis of both the analytic arguments and the numerical computations, we prove that for the family of δ' -regularized potentials with certain configurations, a single bound energy level converges to a finite value, whereas the rest of energy levels escapes to $-\infty$. This is true in general for two families of point interactions, called in the present paper generalized δ - and δ' -potentials, that cover their distributional analogues. The convergence of the multiple bound states under shrinking the finite-thickness double-layer structure to a point behaves according to one of sequences (78) or (79).

Acknowledgments

One of us (AVZ) acknowledges a partial support from the Department of Physics and Astronomy of the National Academy of Sciences of Ukraine (project No. 0117U000240). YZ acknowledges a partial support by the National Academy of Sciences of Ukraine Grant ‘Functional Properties of Materials Prospective for Nanotechnologies’ (project No. 0120U100858). Finally, we are indebted to both Referees for suggestions, resulting in the significant improvement of the paper.

References

- [1] Demkov Y N and Ostrovskii V N 1975 *Zero-Range Potentials and Their Applications in Atomic Physics* (Leningrad: Leningrad University Press)
- [2] Demkov Y N and Ostrovskii V N 1988 *Zero-Range Potentials and Their Applications in Atomic Physics* (New York: Plenum)
- [3] Albeverio S, Gesztesy F, Høegh-Krohn R and Holden H 2005 *Solvable Models in Quantum Mechanics (With an Appendix by Pavel Exner)* 2nd revised edn (Providence: RI: American Mathematical Society: Chelsea Publishing)
- [4] Albeverio S and Kurasov P 1999 *Singular Perturbations of Differential Operators: Solvable Schrödinger-Type Operators* (Cambridge: Cambridge University Press)
- [5] Berezin F A and Faddeev L D 1961 *Sov. Math. Dokl.* **2** 372; translation from *Dokl. Akad. Nauk SSSR* **137** 1011 (1961)
- [6] Kurasov P 1996 *J. Math. Anal. Appl.* **201** 297
- [7] Albeverio S, Dąbrowski L and Kurasov P 1998 *Lett. Math. Phys.* **45** 33
- [8] Albeverio S and Nizhnik L 2003 *Lett. Math. Phys.* **65** 27
- [9] Nizhnik L N 2003 *J. Funct. Anal. Appl.* **37** 85
- [10] Nizhnik L N 2006 *J. Funct. Anal. Appl.* **40** 74
- [11] Albeverio S, Cacciapuoti C and Finco D 2007 *J. Math. Phys.* **48** 032103
- [12] Cacciapuoti C and Exner P 2007 *J. Phys. A: Math. Theor.* **40** F511
- [13] Gadella M, Negro J and Nieto L M 2009 *Phys. Lett. A* **373** 1310
- [14] Brasche J F and Nizhnik L P 2013 *Methods Funct. Anal. Topology* **19** 4

- [15] Kulinskii V L and Panchenko D Y 2015 *Physica B* **472** 78
- [16] Nieto L M, Gadella M, Guilarte J M, Muñoz-Castañeda J M and Romaniega C 2017 *J. Phys. Conf. Series* **839** 012007
- [17] Lange R-J 2012 *J. High Energy Phys.* **JHEP11(2012)** 1
- [18] Lange R-J 2015 *J. Math. Phys.* **56** 122105
- [19] Šeba P 1986 *Rep. Math. Phys.* **24** 111
- [20] Exner P, Neidhardt H and Zagrebnov V A 2001 *Commun. Math. Phys.* **224** 593
- [21] Cheon T and Shigehara T 1998 *Phys. Lett. A* **243** 111
- [22] Christiansen P L, Arnbak N C, Zolotaryuk A V, Ermakov V N and Gaididei Y B 2003 *J. Phys. A: Math. Gen.* **36** 7589
- [23] Zolotaryuk A V, Christiansen P L and Iermakova S V 2006 *J. Phys. A: Math. Gen.* **39** 9329
- [24] Toyama F M and Nogami Y 2007 *J. Phys. A: Math. Theor.* **40** F685
- [25] Zolotaryuk A V 2010 *Phys. Lett. A* **374** 1636
- [26] Zolotaryuk A V and Zolotaryuk Y 2014 *Int. J. Mod. Phys. B* **28** 1350203
- [27] Golovaty Y D and Man'ko S S 2009 *Ukr. Math. Bull.* **6** 169 (e-print arXiv:0909.1034v2 [math.SP])
- [28] Golovaty Y D and Hryniv R O 2010 *J. Phys. A: Math. Theor.* **43** 155204
Golovaty Y D and Hryniv R O 2010 *J. Phys. A: Math. Theor.* 2011 **44** 049802
- [29] Golovaty Y D and Hryniv R O 2013 *Proc. R. Soc. Edinb. A* **143** 791
- [30] Golovaty Y 2013 *Integr. Equ. Oper. Theor.* **75** 341
- [31] Gadella M, Glasser M L and Nieto L M 2011 *Int. J. Theor. Phys.* **50** 2144
- [32] Gadella M, García-Ferrero M A, González-Martín S and Maldonado-Villamizar F H 2014 *Int. J. Theor. Phys.* **53** 1614
- [33] Fassari S, Gadella M, Glasser M L and Nieto L M 2018 *Ann. Phys. (NY)* **389** 48
- [34] Fassari S, Gadella M, Glasser M L and Nieto L M 2018 *Nanosyst. Phys. Chem. Math.* **9** 179
- [35] Fassari S, Gadella M, Glasser M L, Nieto L M and Rinaldi F 2019 *Phys. Scr.* 2019 **94** 055202
- [36] Albeverio S and Nizhnik L 2000 *Ukr. Mat. Zh.* **52** 582
Albeverio S and Nizhnik L 2000 *Ukr. Math. J.* **52** 664
- [37] Albeverio S and Nizhnik L 2007 *J. Math. Anal. Appl.* **332** 884
- [38] Albeverio S and Nizhnik L 2013 *Methods Funct. Anal. Topology* **19** 199
- [39] Albeverio S, Fassari S and Rinaldi F 2013 *J. Phys. A: Math. Theor.* **46** 385305
- [40] Albeverio S, Fassari S and Rinaldi F 2016 *J. Phys. A: Math. Theor.* **49** 025302
- [41] Konno K, Nagasawa T and Takahashi R 2016 *Ann. Phys. (NY)* **375** 91
- [42] Konno K, Nagasawa T and Takahashi R 2017 *Ann. Phys. (NY)* **385** 729
- [43] Calçada M, Lunardi J T and Manzoni L A 2009 *Phys. Rev. A* **79** 012110
- [44] Lunardi J T, Manzoni L A and Monteiro W 2013 *J. Phys. Conf. Series* **410** 012072
- [45] Calçada M, Lunardi J T, Manzoni L A and Monteiro W 2014 *Front. Phys.* **2** 23
- [46] Lee M A, Lunardi J T, Manzoni L A and Nyquist E A 2015 *J. Phys. Conf. Series* **574** 012066
- [47] Lee M A, Lunardi J T, Manzoni L A and Nyquist E A 2016 *Front. Phys.* **4** 10
- [48] Asorey M, García-Alvarez D and Muñoz-Castañeda J M 2006 *J. Phys. A: Math. Theor.* **39** 6127
- [49] Asorey M and Muñoz-Castañeda J M 2008 *J. Phys. A: Math. Theor.* **41** 304004
- [50] Guilarte J M and Muñoz-Castañeda J M 2011 *Int. J. Theor. Phys.* **50** 2227
- [51] Asorey M and Muñoz-Castañeda J M 2013 *Nucl. Phys. B* **874** 852
- [52] Muñoz-Castañeda J M, Guilarte J M and Mosquera A M 2013 *Phys. Rev. D* **87** 105020
- [53] Zolotaryuk A V 2017 *J. Phys. A: Math. Theor.* **50** 225303
- [54] Zolotaryuk A V 2018 *Ann. Phys. (NY)* **396** 479
- [55] Zolotaryuk A V 2019 *Ukr. Fiz. Zh.* **64** 1013
Zolotaryuk A V 2019 *Ukr. J. Phys.* **64** 1021
- [56] Zolotaryuk A V and Zolotaryuk Y 2015 *Phys. Lett. A* **379** 511
- [57] Zolotaryuk A V and Zolotaryuk Y 2015 *J. Phys. A: Math. Theor.* **48** 035302
- [58] Zolotaryuk A V, Tsironis G P and Zolotaryuk Y 2019 *Front. Phys.* **7** 1
- [59] Dodd R K, Eilbeck J C, Gibbon J D and Morris H C 1982 *Solitons and Nonlinear Wave Equations*

(London: Academic Press)

- [60] Heydarov A H 2005 *Baku University Bull.* **3** 21
- [61] Zolotaryuk A V 2010 *J. Phys. A: Math. Theor.* **43** 105302
- [62] Zolotaryuk A V and Zolotaryuk Y 2011 *J. Phys. A: Math. Theor.* **44** 375305
Zolotaryuk A V and Zolotaryuk Y 2012 *J. Phys. A: Math. Theor.* **45** 119501
- [63] Golovaty Y 2012 *Methods Funct. Anal. Topology* **18** 243
- [64] Muñoz-Castañeda J M and Guilarte J M 2015 *Phys. Rev. D* **91** 025028
- [65] Gadella M, Mateos-Guilarte J, Muñoz-Castañeda J M and Nieto L M 2016 *J. Phys. A: Math. Theor.* **49** 015204